Heliyon 10 (2024) e27161

Contents lists available at ScienceDirect

Heliyon

journal homepage: www.cell.com/heliyon

Research article

Scutellaria baicalensis Georgi stems and leaves flavonoids promote neuroregeneration and ameliorate memory loss in rats through cAMP-PKA-CREB signaling pathway based on network pharmacology and bioinformatics analysis

Yinhui Yao [a,b,1], Qianqian Liu [a,1], Shengkai Ding [a], Yan Chen [a], Tangtang Song [a], Yazhen Shang [a,b,*]

[a] *Institute of Traditional Chinese Medicine, Chengde Medical University / Hebei Province Key Research Office of Traditional Chinese Medicine Against Dementia / Hebei Province Key Laboratory of Traditional Chinese Medicine Research and Development / Hebei Key Laboratory of Nerve Injury and Repair, Chengde, China, Chengde, 067000, China*

[b] *Faculty of Integrated Traditional Chinese and Western Medicine, Hebei University of Chinese Medicine, Shijiazhuang, China*

ARTICLE INFO

Keywords:
Scutellaria baicalensis georgi
Flavonoids
Stems and leaves
cAMP-PKA-CREB signaling pathway
Alzheimer's disease
Bioinformatics
Network pharmacology
Neuroregeneration
Memory impairment

ABSTRACT

The aim of this study was to investigate the possible molecular mechanism of *Scutellaria baicalensis* Georgi stems and leaves flavonoids (SSF) in Alzheimer's disease (AD). The active ingredients of SSF and their targets were identified via network pharmacology and bioinformatics analysis. To test the successful establishment of a rat model of AD by $A\beta_{25\text{-}35}$ combined with RHTGF-β_1 and $AlCl_3$, the Morris water maze test was used. To intervene, three different doses of SSF were administered. The model group and the control group were included among the parallel groups. A shuttle box test, immunohistochemistry, an enzyme-linked immunosorbent assay, qPCR and Western blot were performed to verify the results. Based on the intersection of genes among AD disease targets, SSF component targets, and differentially expressed genes in the single cell dataset GSE138852 and bulk-seq dataset GSE5281, nine genes related to the action of SSF on AD were identified. SSF have an important anti-AD pathway in the cAMP signaling pathway. SSF can ameliorate the conditioned memory impairment, augment Brdu protein expression and cAMP content; and differentially regulate the mRNA and protein expressions of GPCR, Gαs, AC1, PKA, and VEGF. The cAMP-PKA-CREB pathway in the SSF may mediate the ability of the SSF to ameliorate the composite-induced memory loss and nerve regeneration in rats induced by composite Aβ.

Abbreviations: AD, (Alzheimer's disease); SPs, (senile plaques); NFTs, (neurofibrillary tangles); RHTGF-β_1, (Recombinant Human Transforming Growth Factor-β_1); SSF, (*Scutellaria baicalensis* Georgi stems and leaves flavonoids); ELISA, (enzyme-linked immunosorbent assays); scRNA-seq, (single-cell RNA sequencing); GEO, (Gene Expression Omnibus); PCs, (principal components); PCA, (principal component analysis); FC, (Fold Change); KEGG, (Kyoto encyclopedia of genes and genomes); DEGs, (differentially expressed genes); WGCNA, (Weighted Gene Co-expression Network Analysis); AARR, (active avoidance response rate); GARR, (general avoidance response rate); AARL, (active avoidance latency); PARL, (passive avoidance latency); ANOVA, (one-way analysis of variance); BP, (biological processes); CC, (cellular components); MF, (molecular functions); SVZ, (subventricular zone); SGZ, (subgranular zone).

* Corresponding author. Institute of Traditional Chinese Medicine, Chengde Medical University, Chengde, China.
E-mail address: 973358769@qq.com (Y. Shang).

[1] These authors have contributed equally to this work.

https://doi.org/10.1016/j.heliyon.2024.e27161
Received 22 October 2023; Received in revised form 23 February 2024; Accepted 26 February 2024
Available online 27 February 2024

1. Introduction

The aging-related neurodegenerative disease Alzheimer's disease (AD) has clinical manifestations such as cognitive and memory impairment, personality changes, and behavioral changes [1]. As a result of the excessive aggregation of amyloid β-proteins, which results in the formation of senile plaques (SPs), the overphosphorylation of tau protein which results in neurofibrillary tangles (NFTs), neuroinflammation, and synaptic abnormalities, is a prominent pathological feature of AD [2]. Neuronal loss or death as a result of the

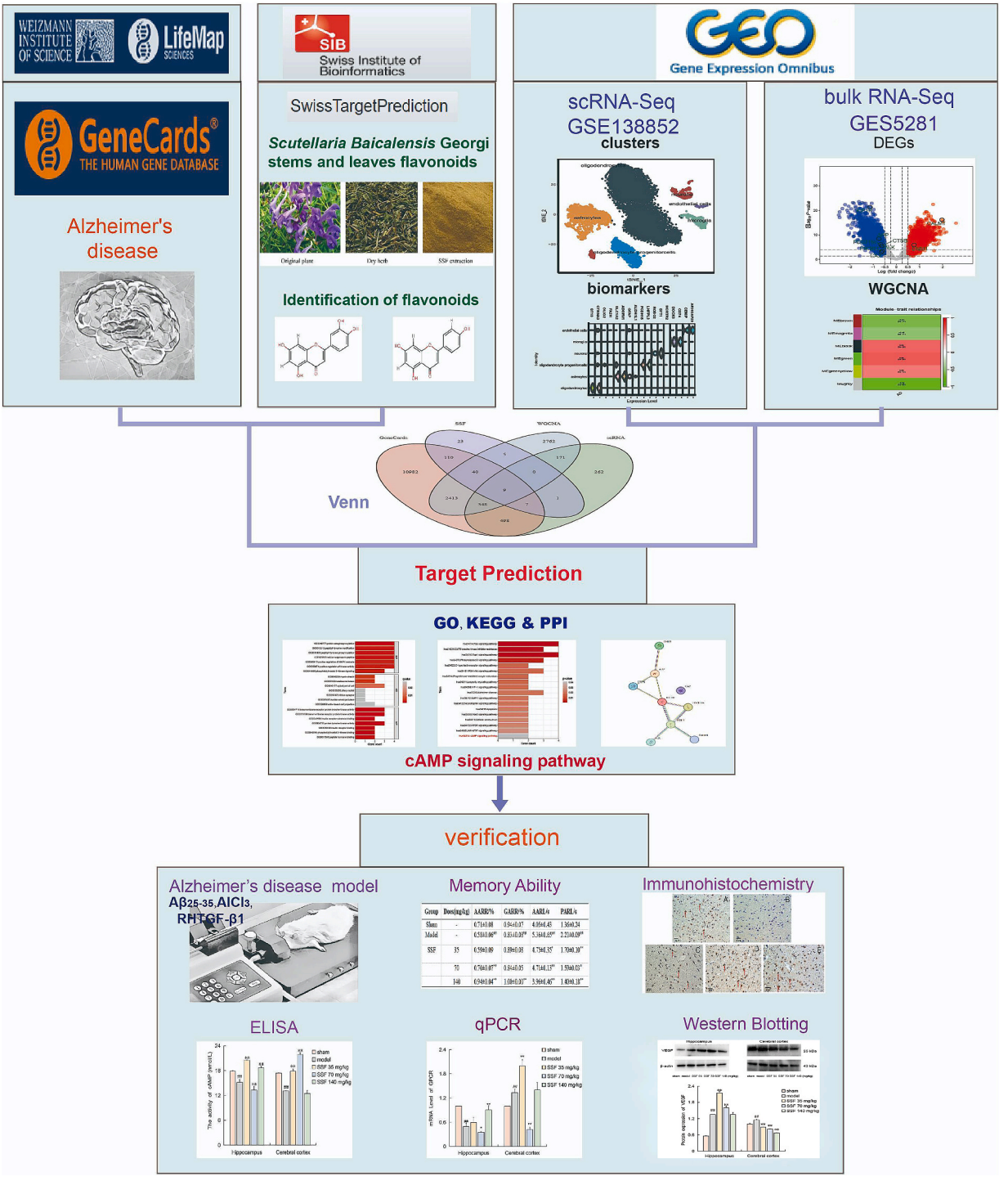

Fig. 1. A flow chart of the study.

pathological changes mentioned above affects learning and memory, causing cognitive impairment in patients with AD [3]. The process of neuroregeneration involves the migration, proliferation, differentiation, and maturation of neural stem cells to generate neurons. As a result, neurodegeneration is promoted and neuron loss is reduced [4]. Several signal transduction pathways are implicated in the regulation of neuroregeneration, including the cAMP-PKA-CREB signaling pathway, are implicated in the regulation of neuroregeneration[5,6]. There is evidence linking cAMP-PKA-CREB signaling to neuroregeneration, memory formation, synaptic plasticity, and neuronal function, suggesting that this pathway is a potential target for the treatment of neurological disorders[7–9]. Hence, investigating the regulation of the cAMP-PKA-CREB signaling pathway for neuroregeneration may help improve memory loss and screen therapeutic drugs for AD patients.

The traditional Chinese herbal medicine *Scutellaria baicalensis* Georgi contains flavonoids that act as antioxidants, anti-inflammatory agents, and immune stimulants [10]. The stems and leaves of *Scutellaria baicalensis* Georgi contain 21 composites, the best-known of which are baicalin, scutellarin, luteolin, apigenin and pinocembrin [11]. In AD animal models, *Scutellaria baicalensis* Georgi stems and leaves flavonoids (SSF) are increasingly demonstrated to have therapeutic effects [12–14]. The biological activity of SSF have been extensively studied, but its mechanism of action in treating AD has not been determined. Notably, the cAMP-PKA-CREB signaling pathway has not been described.

Recent research on drugs and diseases has made use of network pharmacology and bioinformatics [15–17]. Through a network analysis of diseases, drugs and targets, multiple dimensions of the relationships between Chinese herbal medicine targets and genes and between these factors and signaling pathways were revealed. Moreover, RNA-seq technology, as well as sequencing technologies, has been used to analyze gene expression patterns in different populations in recent years [18]. The transcriptome provides information directly related to cell phenotypes, which is helpful for understanding disease mechanism changes. The anti-AD effects of SSF were studied in this study using bioinformatics methods, including microarray data analysis, single cell transcriptomics, and network pharmacology (Fig. 1). First, SSF were used to screen potential target genes, and AD-related target genes were subsequently identified. Following microarray data analysis and single cell transcriptomics, we identified the differentially expressed genes. The second step will be to identify the gene targets of the SSFs as those related to AD. Finally, we established a model of AD-like memory impairment in rats by intraventricular injection of $A\beta_{25\text{-}35}$ combined with $AlCl_3$ and Recombinant Human Transforming Growth Factor-β_1 (RHTGF-β_1). For detection and verification of mRNA and protein expression in the predicted signal pathway, shuttle boxes, immunohistochemistry, enzyme-linked immunosorbent assays (ELISA), qPCR and Western blotting were used. As a result of our research, we have developed a more specific and effective treatment method and we have gained new insight into how SSF can be used to treat AD (see Fig. 2).

2. Materials and methods

2.1. Target screening of flavonoids from Scutellaria baicalensis georgi stems and leaves

According to previous studies, 21 different flavonoids from *Scutellaria baicalensis* Georgi stems and leaves were reported, and the results are shown in Table S1. Through these known drug components, the corresponding targets of the drug components can be predicted. Specifically, the drug components were input into the SwissTargetPrediction database (http://www.swisstargetprediction.ch/), the conditional probability was set to greater than 0.1, and the potential targets of the drug components were selected for subsequent analysis [19].

2.2. Target screening of Alzheimer's disease

With respect to the GeneCards Version 5.16 database (https://www.genecards.org/), the disease targets of AD were searched by using the keyword "Alzheimer's disease".

2.3. Data processing for single-cell RNA sequencing

The single-cell RNA sequencing (scRNA-seq) dataset GSE138852 was analyzed using the Seurat software package in R software as part of the Gene Expression Omnibus (GEO) project (http://www.ncbi.nlm.nih.gov/geo)[20].There were six human tissue samples

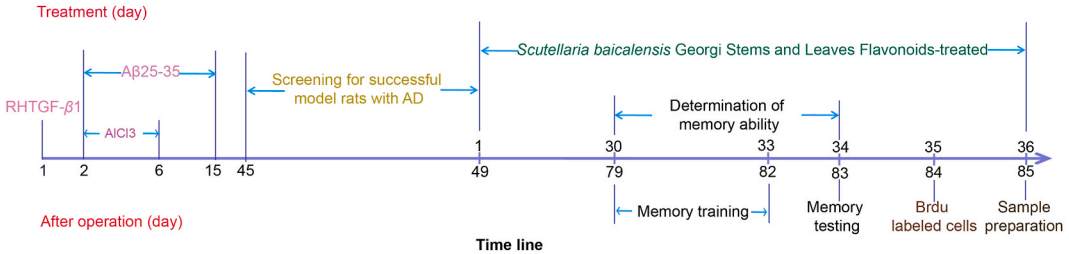

Fig. 2. Timetable for animal experimental design.

included in this dataset, three belonging to the control group and three belonging to the AD group. The platform used for the measurements was an Illumina NextSeq 500 (*Homo sapiens*) from GPL18573.It is used in single cell transcriptomics to filter, normalize, reduce dimensionality, and cluster cells using Seurat package [21]. The "Log2Normalize" method standardizes gene expression in single cells. In addition to identifying significant principal components (PCs) via principal component analysis (PCA), the FindClusters function was subsequently used to classify cells, and CellMarker 2.0 (http://www.bio-bigdata.center/) was subsequently used to annotate the cells.Using the Harmony package, a batch effects between samples were eliminated. The FindAllMarkers function, which uses a log Fold Change (FC).threshold = 0.25, was used to identify differentially expressed genes (DEGs) in each cluster. Finally, the DEGs of each cluster were analyzed by the Kyoto encyclopedia of genes and genomes (KEGG).

2.4. Data processing for bulk RNA-seq

The GSE5281 dataset was obtained from the GEO database and included 74 controls and 87 AD patients[22]. The samples were taken from the human brain. The GPL570 platform was used to analyze the data. Using Limma, differentially expressed genes (DEGs) were identified based on the $|\log FC|>0.5$ and $P < 0.05$ thresholds[15]. After that, Weighted Gene Co-expression Network Analysis (WGCNA) was used to determine whether any genes related to AD were present in the expression matrix containing the differentially expressed genes [16,23]. A disease-related gene network module can be constructed using what is known as WGCNA, a powerful tool for bioinformatics. To generate the weighted adjacency matrix, the Pearson correlation coefficient of each gene pair was calculated. As a result of determining the soft threshold, the constructed network is more consistent with the characteristics of a scale-free network. The genes were subsequently identified in different gene modules using the soft threshold parameter in accordance with the appropriate power. To construct a coexpression network, at least 50 genes were needed for each gene module. The module associated with the phenotype of interest was identified by analysing the relationship between each network module and the sample phenotype. It is possible to identify modules that are highly correlated with AD by calculating the correlation between modules and phenotypes. In this study, we will display modular genomes that are strongly associated with AD.

2.5. Targets related to disease drugs

The above analysis revealed the targets of flavonoids in *Scutellaria baicalensis* Georgi stems and leaves, targets related to AD diseases, differentially expressed genes according to single cell transcriptomics and genes related to the AD phenotype via WGCNA these genes were intersected for subsequent analysis. The results were visualized with the VennDiagram of R package. The genes obtained by the intersection of the above four methods are called common genes.

2.6. Functional annotation, pathwayenrichment analysis and protein–protein interaction network construction

With respect to the R software, clusterProfiler and org.Hs.eg.db were used to analyze gene ontology (GO) annotation and KEGG pathway enrichment analyses of intersecting genes, and $P < 0.05$ was considered to indicate a statistically significant difference [24]. The target genes at the intersection of common genes were imported into the STRING database (http://string-db.org) to construct a protein–protein interaction (PPI) network [25]. The "*Homo sapiens*" was specified as the species in the operation interface, while "0.4″ was set as the confidence score.

2.7. Animals

The Beijing Vital River Laboratory Animal Technology Co., Ltd. provided us with sixty healthy male SPF Wistar rats (260–300 g, Certification NO SCXK (jing) 2016-1-0006). It is important to mention that the rats were allowed free access to food and water at Chengde Medical University's Experimental Animal Center. Five rats were housed in each cage, and the laboratory conditions were as follows: 40%–60% relative humidity, 24–26 °C ambient temperature, and 12-h light-dark cycles. In all the experiments, the animals were handled in accordance with the ethics guidelines of Chengde Medical University's Animal Ethics Committee (NO.CDMULAC-20 190226-002). Animals were subjected to all possible measures to reduce their discomfort and the number of animals used in the research.

2.8. Instruments and reagents

The 68000 Brain Stereotaxic apparatus was supplied by Shenzhen RWD Life Science and Technology Co., Ltd; The Institute of Medicine, Chinese Academy of Medical Sciences supplied the Morris water maze. An XR-XC105 shuttle box (480 × 240 × 300 mm) was purchased from Shanghai Xin Ruan information Technology Co., Ltd. Optical microscopy was obtained from OLYMPUS Company, Japan. It was provided by ALPHA Company, America, used an IMAGER550 gel image analysis system. The American Agilent Company provided the Mx3000P and StrataGene quantitative PCR instruments.

SSF were obtained from the Institute of Chinese Medicine, Chengde Medical College (purity, 88.6%) [26]. $A\beta_{25\text{-}35}$ (Lot. MB10445) was obtained from Dalian Meilun Biotechnology Co., Ltd. $AlCl_3$ was obtained from Tianjin Beichen Chemical Reagent Co., Ltd. RHTGF-β_1 was afforded by PEPROTECH Company. Brdu (Lot. BM0201) antibody was purchased from BOSTER Company. $A\beta_{25\text{-}35}$ was diluted to a concentration of 1 μg per milliliter using a 0.9% NaCl solution. To prepare RHTGF-β_1 at a concentration of 10 ng/μL, 100 μL of citric acid and 900 μL of PBS were utilized. The $AlCl_3$ mixture was composed of ultrapure water containing 1%. GPCR, Gαs, AC1,

VEGF primers were purchased from TaKaRa Company. Screen QuesTM Colorimetric ELISA Camp Assay Kit was supplied by Dakewe Biotech Co., Ltd. The antibodies PKA (Lot.BS1576) and AC1 (lot. BS2391) were acquired from Bioworld Company. The antibody of Gαs (Lot. bs3939R) was provided by Bioss Company. It is made of antibodies VEGF (Lot. AF5131) and GPCR (Lot. ab136331) obtained from Affinity Company.

2.9. Surgical procedure

Sixty Wistar rats were randomly divided into two groups: one group underwent a sham operation (n = 10) and the other group underwent a surgical operation (n = 50). Anaesthetized rats were fixed with isoflurane on brain stereotaxic instruments, the meninges were removed, the skull was fully exposed, and three points were marked at bregma. RHTGF-β_1 (10 ng/μL) was microinjected at the first time point (2 mm behind the bregma, 1.4 mm left of the sagittal suture, and 4.6 mm below the skull), and the dose was one μl. On the second day after the operation, 4 μg (1 μL) of $A\beta_{25\text{-}35}$ and 3 μL of $AlCl_3$ (1%) were microinjected at the second point (0.8 mm behind the bregma, 2.0 mm left the sagittal suture and 4.6 mm below the skull) through a catheter for 14 days in the morning and 5 days in the afternoon, respectively. To fix the remaining two points, we used the third point (2.0 mm before the bregma and 1.5 mm on the left of the sagittal suture) in a triangle with the other two points. The rats in the sham operation group were microinjected with the same volume of 0.9% NaCl into the lateral cerebral ventricle. To cover the skin incision, fix the catheter, and prevent postoperative infections, the denture base and denture base water were thoroughly mixed. The incision was sutured after the microinjection was completed. During the whole period, the rats were kept under observation [27].

2.10. Model selection, grouping, and administration of SSF to rats

All rats were subjected to Morris water maze training on day 45 after the operation to determine whether the AD model was successful. The latency of the rats to find the platform was measured during training. In the model screening index, the average latency of day 4 was used in place of the training four times a day for four days. Finally, this study showed that the memory impairment of the rats was 81.25% successful. Using the success rate of the rats, three groups were randomly established (35, 70, and 140 mg/kg of SSF). The SSF solution was intragastrically administered for 30 days to the rats in the drug group at doses of 35, 70, and 140 mg/kg. A 0.9% NaCl solution was given to rats in both the model group and the sham group.

2.11. Determination of memory ability

After 79 days following surgery, the rats passed the conditioned learning and memory test via the XR- XC105 shuttle box experiment and video analysis system, which is equivalent to the method used 31 days after treatment with SSF. At the beginning of training, the rats were allowed to move freely in the box for 3 min to eliminate the inquiry reflex, followed by conditioned stimulation for 10 s. The rats were subsequently shuttled to the contralateral compartment during conditioned stimulation, after which the stimulation ended, which was recorded as an active avoidance response (AAR). If the rats did not shuttle to the contralateral compartment, followed by 0.8 mA unconditioned stimulation for 5 s, and the rats shuttled to the contralateral safe area to end the electric shock, the response was recorded as a passive avoidance response (PAR), otherwise, the response was recorded as no response. The abovementioned process continued as a cycle. The stimulation was repeated at an intervals of 10 s, 20 times a day for 5 consecutive days, with the first 4 days considered training and the 5th day considered testing. Moreover, the active avoidance response rate (AARR), general avoidance response rate (GARR), active avoidance latency (AARL), and passive avoidance latency (PARL) were also recorded.

2.12. Sample preparation

A total of 50 mg/kg of Brdu50 was administered three times with at 4-h intervals on the 83rd day after surgery, which was the day 35 of the SSF treatment. After 36 days of SSF treatment, the rats were decapitated the 84 days after the operation, after which the plants were administered and injected with SSF for the final time. For immunohistochemistry, the right hemispheres of four rats were fixed in 4% paraformaldehyde for 24 h and embedded in paraffin wax. The separated rat brain samples were stored at −86 °C, after which ELISA, qPCR, and protein blot analyses were conducted.

2.13. Detection of brdu protein expression by immunohistochemistry

Immunohistochemistry was performed on the paraffin sections according to the previous methods [28]. In rats divided into three sections, Brdu was found in cerebral cortex cells. The cells appear as brown particles under a microscope. The tissues from each group of rats were been divided into three sections and six visual fields were taken under the microscope (400 ×). The percentage was calculated based on the number of Brdu-positive cells.

2.14. Detection of cAMP content by ELISA

The hippocampal and cerebral coetex cAMP concentrations were determined using an ELISA kit in strict accordance with the manufacturer's instructions. Test samples were taken from tissue supernatants. Standard curves were constructed by using standards

with different concentrations and absorbance values, and cAMP concentrations were calculated for each group.

2.15. mRNA expression levels of GPCR, gαs, AC1, and VEGF in rats determined via qPCR

Total RNA was extracted from the hippocampus and cerebral cortex of the rats regions using the Trizol method. The DNA from the genomic samples was removed and reverse transcribed using a reverse transcription kit after which cDNA was synthesized. The primers used for qPCR in this study can be found in Table S1. The cDNA was amplified using the TB Green™ Premix Ex Taq™ II kit. The PCR procedure was as follows: 95 °C for 30 s, 95 °C for 5 s, and 60 °C for30 s, for 40 cycles. The ct value and amplification dissolution curve were obtained. The target mRNA expression relative to that of β-actin was assessed by the $2^{-\triangle\triangle Ct}$ method. The following formula was used for calculation: F = 2-((average Ct value of target gene− average Ct value of β-actin in the model group or the three-dose SSF group)-(average Ct value of target gene− average Ct value of β-actin in the sham-operated group)).

2.16. Protein expression levels of GPCR, gαs, AC1, PKA, and VEGF in rats determined via western blotting

Research papers prior to this study have detailed how these factors were extracted and measured in the hippocampus and cortex, respectively [28]. Image J software was used to analyze the above-mentioned protein bands. Three rats (hippocampus and cerebral cortex regions of the brain) from each group were assessed for their brains, and each rat was tested three times to verify the findings. Gray ratio analysis was used to analyze target protein expression relative to that of the internal reference protein (*β*-actin).

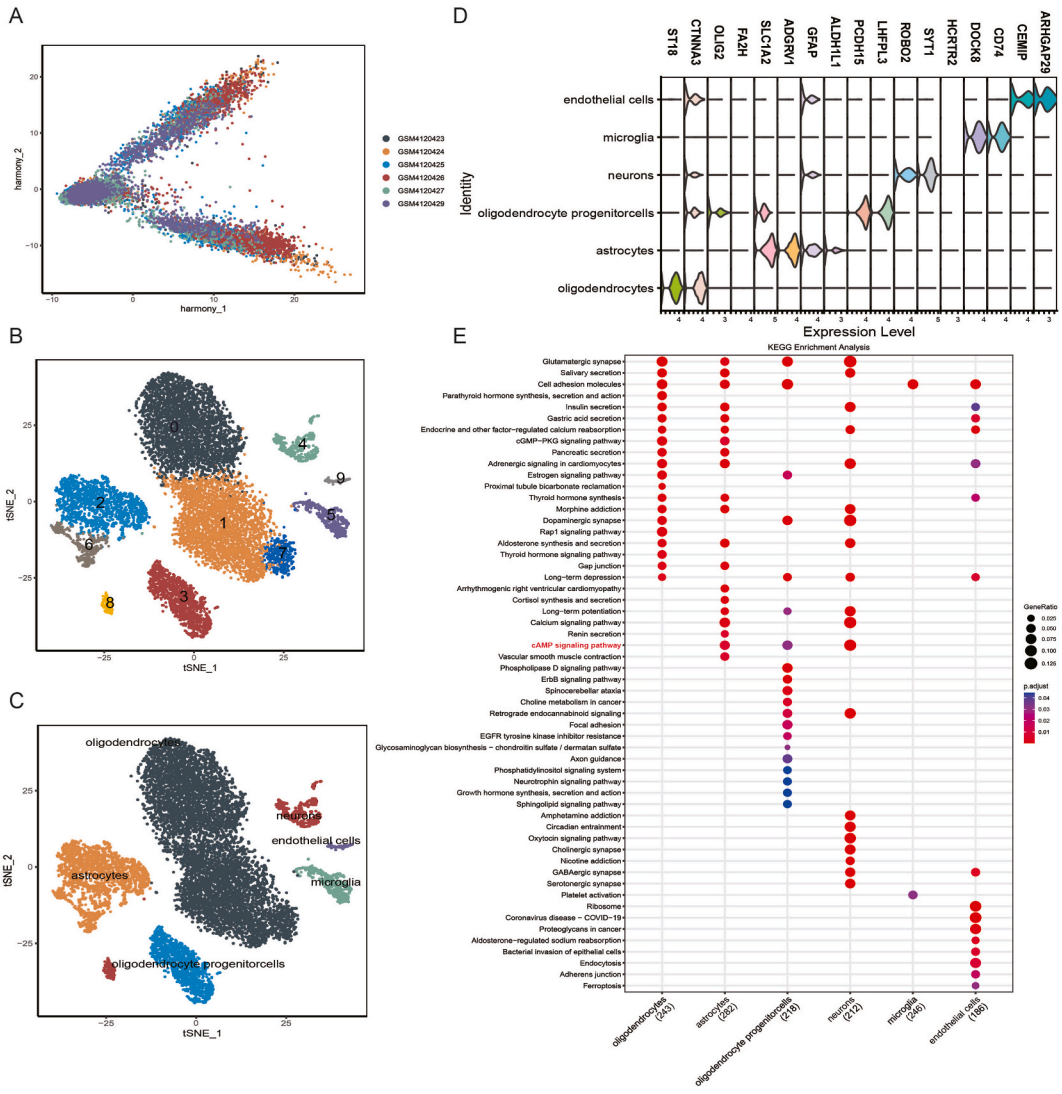

Fig. 3. Gene expression analysis on scRNA sequencing.

2.17. Statistical analysis

To analyze all the data, we used SPSS 21.0 statistical software. The results are presented as the mean ± SD. The means of different samples were analyzed using one-way analysis of variance (ANOVA). In the absence of normality, a Kruskal-Wallis test was conducted. The bioinformatics data in this study were analyzed with R software (version 4.1.3). The significance level was set at $P < 0.05$.

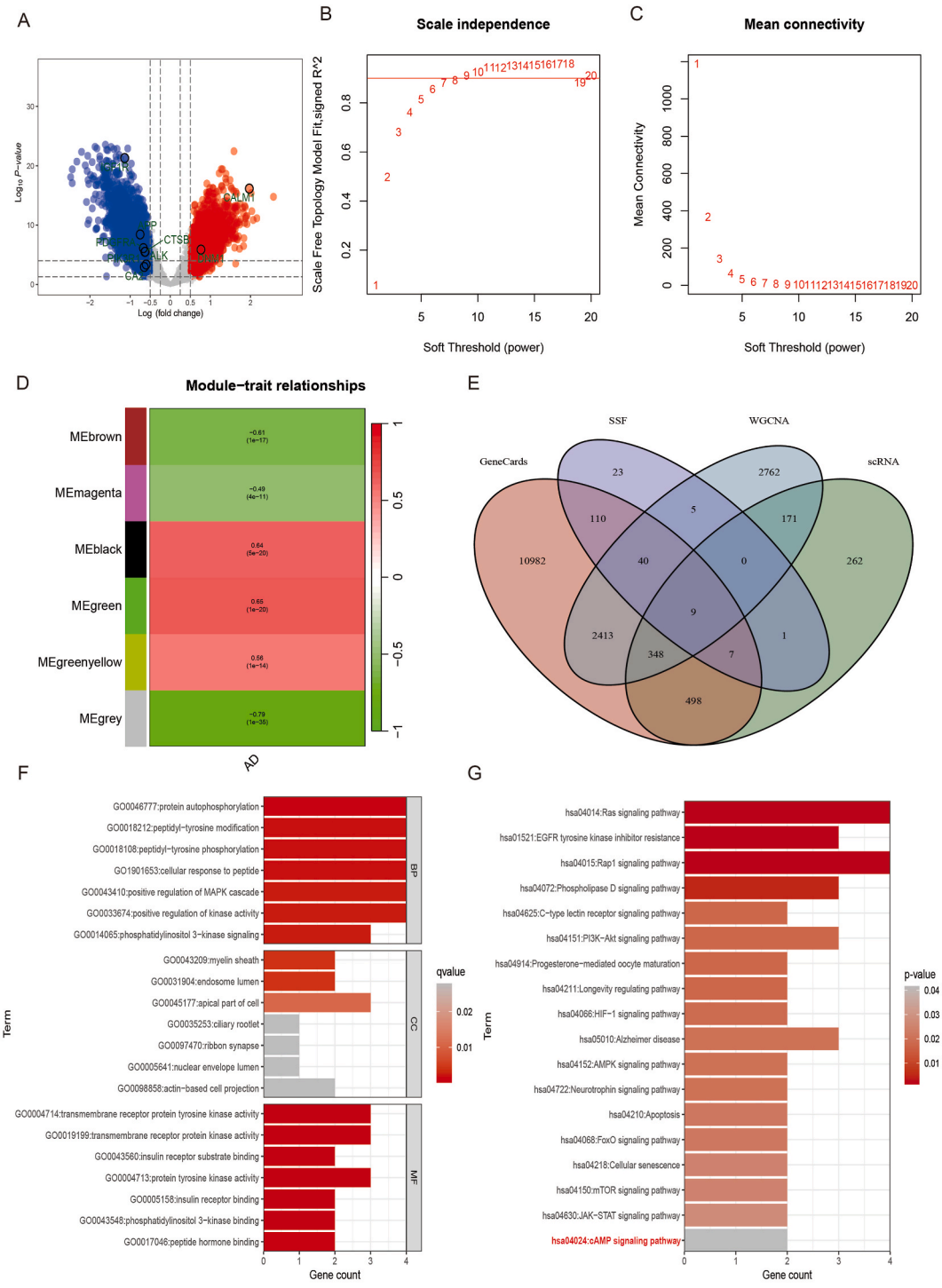

Fig. 4. Gene expression analysis on bulk RNA-seq and target-related signaling pathway.

3. Results

3.1. Potential drug targets

Five hundred and sixty-nine potential targets were obtained by screening 21 flavonoids of SSF from SwissTargetPrediction (Table S2), and 200 targets were removed following duplication (Fig. 4E).

3.2. Disease target screening

A total of 14408 AD-related targets were screened from the GeneCards database (Fig. 4E–Table S3).

3.3. DEGs from scRNA sequencing

The initial quality filtering was performed using Seurat, and each gene had to be expressed in at least three cells, and each cell had to express at least 200 genes and no more than 1500 genes. It appears that less than 3% of the cells have mitochondria. A total of 13,214 cells were filtered down to 12713 cells. Using FindVariableFeatures, highly variable genes in single cells were identified. Principal component analysis (PCA) was performed on all the genes, and the batch effect between samples was determined via the harmony package (Fig. 3A). In the R package of Seurat, FindNeighbors and FindClusters are used to cluster cells, with the resolution set to 0.3. We used the tSNE method to identify six cell types, namely, oligodendrocytes (expressing ST18, CTNNA3, OLIG2 and FA2H), astrocytes (expressing SLC1A2, ADGRV1, GFAP and ALDH1L1), oligodendrocytes progenitorcells (expressing PCDH15 and LHFPL3), neurons (expressing ROBO2, SYT1 and HCRTR2), microglia (expressing DOCK8 and CD74), and endothelial cells (expressing CEMIP and ARHGAP29) (Fig. 3B&C). FindAllMarkers were used to identify the characteristic genes in a cell population (Fig. 3D). There were 3115 genes differentially expressed among the different types of cells (Table S4), and the number of genes after duplication was reduced to 1296. The marker genes of the 6 subgroups were subsequently subjected to KEGG annotation via the clusterProfiler package (Fig. 3E). The signaling pathways of the different cells are shown in Fig. 3E. The cells in which the cAMP signaling pathway is activated include astrocytes, oligodendrocyte progenitor cells and neurons.

3.4. DEGs from bulk RNA-seq

After analyzing the DEGs in the GSE5281 dataset, 6119 DEGs were screened out according to the screening conditions. Among these genes, 3068 were upregulated, and 3051 were downregulated (Fig. 4A). To determine which genes are related to AD, the co-expression gene modules were screened based on the expression of 6119 genes via WGCNA with the power of a soft threshold of 8 (Fig. 4B&C), and finally six different gene modules were ultimately identified, among which three gene modules were related to clinical trait AD ($r > 0.5$, $P < 0.001$). A total of 5748 genes were obtained from these three gene modules (Fig. 4D).

3.5. Common genes

Using the following four different processes, we identified disease targets associated with SSF. After these genes were crossed, nine common key genes were identified as follows: APP, CTSB, PIK3R1, IGF1R, PDGFRA, ALK, CALM1, CA2 and DNM1 (Fig. 4E). Fig. S1 shows where these nine genes are distributed and how they are expressed in different nerve cells. Many genes are expressed throughout all cells, but the APP gene appears to be the most prevalent. In addition to being expressed in oligodendrocyte progenitorcells, CALM1 is expressed in many other cells. The other seven genes are expressed only in specific types of cells.

3.6. Functional annotation, pathway enrichment analysis and PPI network of the key genes

According to the GO analysis of these nine key genes, the enriched biological processes (BP) terms included protein autophosphorylation, cellular response to peptide and peptidyl-tyrosine phosphorylation; The enriched cellular components (CC) terms included the myelin sheath, endosome lume and apical part of cell; The enriched molecular functions (MF) terms included transmembrane receptor protein tyrosine kinase activity, insulin receptor substrate binding and phosphatidylinositol 3-kinase binding (Fig. 4F). In addition, KEGG enrichment analysis revealed the Rap1 signaling pathway, Ras signaling pathway, and cAMP signaling pathway (Fig. 4G). A PPI network was constructed by entering nine common targets into the STRING database and constructing a PPI network that included 9 edges and 9 nodes (Fig. S2).

3.7. Impact of the SSF on the memory of rats

As surgical modeling of AD in rats has a success rate of 75%, there were 6 animals in each group in this study. As shown in Table 1, rats were intracerebroventricularly injected with the composite Aβ agent, which had significantly decreased the AARR, and GARR, but significantly increased the AARL and PARL. Compared with those in the sham operation group, the AARR and GARR in the model group decreased were 18.31% and 11.7% lower ($P < 0.01$), respectively, but the AARL and PARL were 32.35% ($P < 0.01$) and 62.5% greater ($P < 0.01$) respectively. However, this was an interesting finding. The changes in AARR, GARR, AARL and PARL in rats were reversed after 35, 70 and 140 mg/kg SSF. Compared with those in the model group, the AARRs in the SSF-treated group were

proportionally greater. This study revealed that as rats were administered increasing doses of SSF (35.7 mg/kg, 70 mg/kg, 140 mg/kg), the AARR increased by 1.7%, 20.69%, and 62.07%, respectively ($P < 0.01$). PARL increased by increase of 1.7% ($P > 0.01$), 20.69% ($P < 0.01$) and 62.07% ($P < 0.01$), respectively. In contrast to the increase in the dose of SSF, the PARL decreased by 23.08% ($P < 0.01$), 28.05% ($P < 0.05$) and 36.65% ($P < 0.01$), respectively. Similar results were found for the results in AARL, in which there were 11.38% ($P < 0.05$), 12.13% ($P < 0.01$) and 26.12% ($P < 0.01$) reductions, respectively. However, the GARR was not proportional to the dose of SSF, and a statistically significant increase (32.53%, $P < 0.01$) was found only with high doses of SSF.

3.8. SSF affects brdu protein expression in the rat cortex

As shown in Fig. 5 and Table 2, the increase in the protein expression of BrdU was detected by the brown particle staining (↑) which was mainly present in the cytoplasm and to some extent in the nucleus. Fig. 5 (A and B) shows that, compared with that in the sham operation group, the percentage of Brdu-positive cells was significantly lower (81.08%) ($P < 0.01$). The positive expression of Brdu was reversed by intracerebroventricular injection of composited Aβ after 36 days of SSF treatment. Compared to those in the model group, as shown in Fig. 5 (C, D, and E), the number of neurons in the three-dose SSF group were greater, the nuclear morphology was more normal, the color of the brown granules was more pronounced, and the Brdu expression in the cerebral cortex was increased by 385.71% ($P < 0.01$), 478.57% ($P < 0.01$) and 407.14% ($P < 0.01$) in response to 35, 70 and 140 mg/kg of SSF, respectively.

3.9. Impact of the SSF on the cAMP concentration in rats

Fig. 6 shows that the intracerebroventricular injection of the composite Aβ agent into rats decreased cAMP levels. In the Model group, cAMP levels were attenuated by 14.90% in the hippocampus and 24.93% in the cerebral cortex relative to those in the sham group. Three doses of SSF were administered intragastrically for 36 days, but the cAMP levels changed to varying degrees. The SSF content increased by 35 and 140 mg/kg in comparison with that in the model group (35.05%, $P < 0.01$) and 122.75%, $P < 0.01$, respectively), compared to that in the model group. In contrast, 70 mg/kg SSF reduced the cAMP concentration in the hippocampus by 12.23% ($P < 0.01$) compared to that in the model group. On the other hand, 35 and 70 mg/kg SSF increased the cAMP concentration in the cerebral cortex by 36.44% ($P < 0.01$) and 67.13%, respectively. Additionally, the cerebral cortex cAMP concentration did not change when 140 mg/kg SSF was administered.

3.10. The influence of SSF on cAMP-PKA-CREB signaling pathway mRNA and protein expression in rats

3.10.1. Rat GPCR mRNA and protein expression in response to SSF

Fig. 7A shows the expression of GPCR mRNA in the hippocampus and cerebral cortex of the rats. A comparison between the model group and the sham operation group revealed that GPCR mRNA expression in the hippocampal region decreased by 50.77% ($P < 0.01$) and increased by 33.07% ($P < 0.01$). In contrast, three doses of SSF administered intragastrically for 36 days regulated GPCR mRNA expression to varying degrees. Compared to that in the model group, the expression of GPCR mRNA in the hippocampus was increased by 20.68% ($P < 0.0$l) and 49.89% (cerebral cortex, $P < 0.01$) in the 35 mg/kg of SSF treatment group; by 28.78% (hippocampus, $P < 0.05$) and 68.46% (cerebral cortex, $P < 0.01$) in the 70 mg/kg SSF, treatment group; and by 83.14% (hippocampus, $P < 0.01$) and 5.17% (cerebral cortex, $P > 0.01$) in the 140 mg/kg of SSF treatment group.

According to Fig. 7B, in the model group, GPCR protein expression decreased by 10.23% in the hippocampal region and 10.79% in the cerebral cortex compared to that in the sham operation group ($P < 0.05$). Treatment with 140 mg/kg SSF for 36 days led to a 28.09% increase in GPCR protein expression compared to that in the model group ($P < 0.001$). Neither 35 mg/kg nor 70 mg/kg SSF significantly altered GPCR protein expression in the hippocampus compared with that in the same model group. SSF administration at 35, 70, and 140 mg/kg increased the expression of GPCR proteins in the cerebral cortex by 5.8%, 11.27% ($P < 0.01$), and 5.96%, respectively.

3.10.2. Rat gαs mRNA and protein expression in response to SSF

It can be seen from Fig. 8A that intracerebroventricular injection of composite Aβ is associated with a reduction in the expression of Gαs mRNA in rats. Compared with that in the sham group, the expression of Gαs mRNA in the model group decreased by 9.87% (hippocampus, $P < 0.05$) and 1.26% (cerebral cortex, $P > 0.05$), respectively. After three different doses of SSF were administered for 36 consecutive days, compared with the model group, the mRNA of Gαs in 35 mg/kg group decreased by 11.94% ($P < 0.05$) and

Table 1
Impact of SSF on AARR, GARR, AARL, and PARL as assessed by the shuttle box experiment on rats treated with composited Aβ (mean ± SD, n = 6).

Group	Does(mg/kg)	AARR/%	GARR/%	AARL/s	PARL/s
Sham	–	0.71 ± 0.08	0.94 ± 0.07	4.05 ± 0.43	1.36 ± 0.24
Model	–	0.58 ± 0.06$^{\#\#}$	0.83 ± 0.08$^{\#\#}$	5.36 ± 0.65$^{\#\#}$	2.21 ± 0.09$^{\#\#}$
SSF	35	0.59 ± 0.09	0.89 ± 0.08	4.75 ± 0.35*	1.70 ± 0.10**
	70	0.70 ± 0.07**	0.84 ± 0.05	4.71 ± 0.13**	1.59 ± 0.03*
	140	0.94 ± 0.04**	1.00 ± 0.00**	3.96 ± 0.46**	1.40 ± 0.18**

Note: $^{\#\#}P < 0.01$ vs sham group, $^{**}P < 0.01$ vs model group.

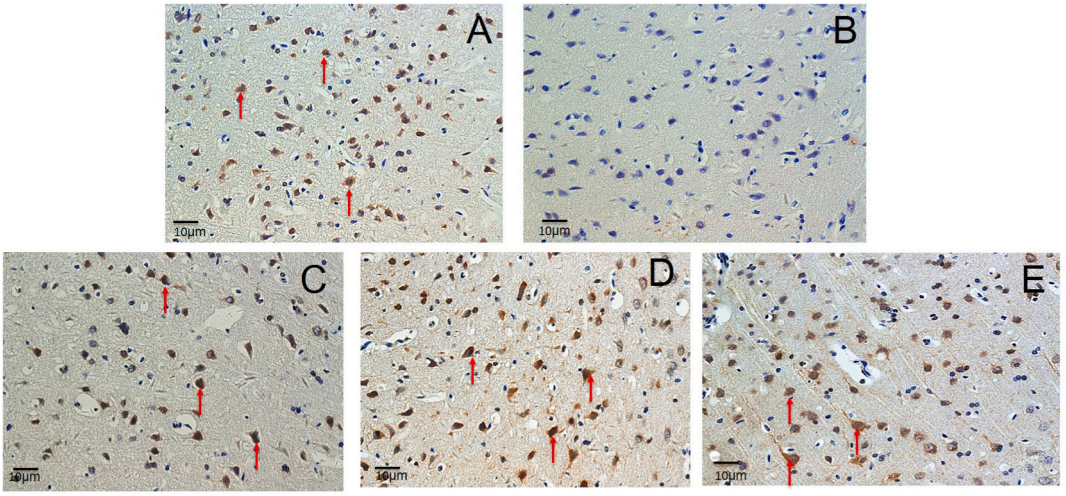

Fig. 5. Rats treated with composited Aβ and SSF expressed Brdu in their cerebral cortex. A: sham group; B: model group; C: SSF 35 mg/kg group; D: SSF 70 mg/kg group; and E: SSF 140 mg/kg group. The positive expression of Brdu protein is shown by the brown particle staining (↑), and the three doses of SSF increased the number of positive cells (400 ×). (For interpretation of the references to color in this figure legend, the reader is referred to the Web version of this article.)

Table 2
SSF effects on Brdu-positive neurons in rats treated with composited Aβ (mean ± SD, n = 6).

Group	Does(mg/kg)	Brdu positive expression Cells in the cerebral cortex/%
Sham	–	0.74 ± 0.15
Model	–	0.14 ± 0.64$^{\#\#}$
SSF	35	0.68 ± 0.22**
	70	0.81 ± 0.97**
	140	0.71 ± 0.27**

Note: $^{\#\#}P < 0.01$ vs sham group; $^{**}P < 0.01$ vs model group.

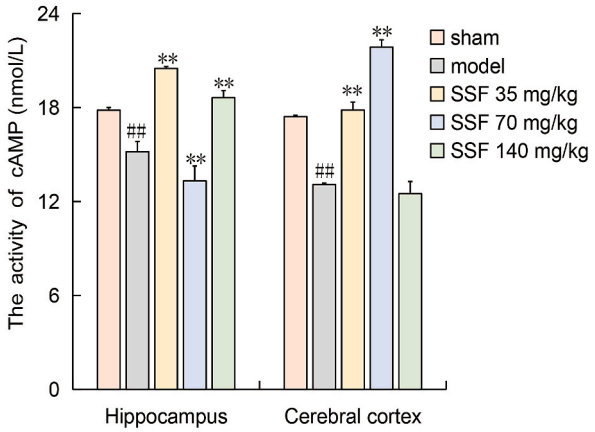

Fig. 6. The effect of SSF on cAMP content in the hippocampus and cerebral cortex of rats exposed to composite Aβ. Mean ± SD. n = 3. $\#\#P < 0.01$ vs sham group; $^{**}P < 0.01$ vs model group.

36.92% ($P < 0.0$l) in hippocampus and cerebral cortex, respectively; the mRNA of Gαs (70 mg/kg group) decreased by 8.11% ($P > 0.01$)and 19.58% ($P < 0.01$) in hippocampus and cerebral cortex, respectively; Gαs mRNA (140 mg/kg group) reduced by 8.11% ($P < 0.01$) and 19.58% ($P < 0.01$), respectively, in the hippocampus and cerebral cortex.

As shown in Fig. 8B, compared with that in the sham operation group, the expression of the Gαs protein in the model group was 14.81% lower (hippocampus, $P < 0.01$) and 20.83% lower (cerebral cortex, $P < 0.01$) than that in the sham operation group. After 36 days of intragastric administration of three different doses of SSF, the hippocampus and cerebral cortex of the rats expressed different

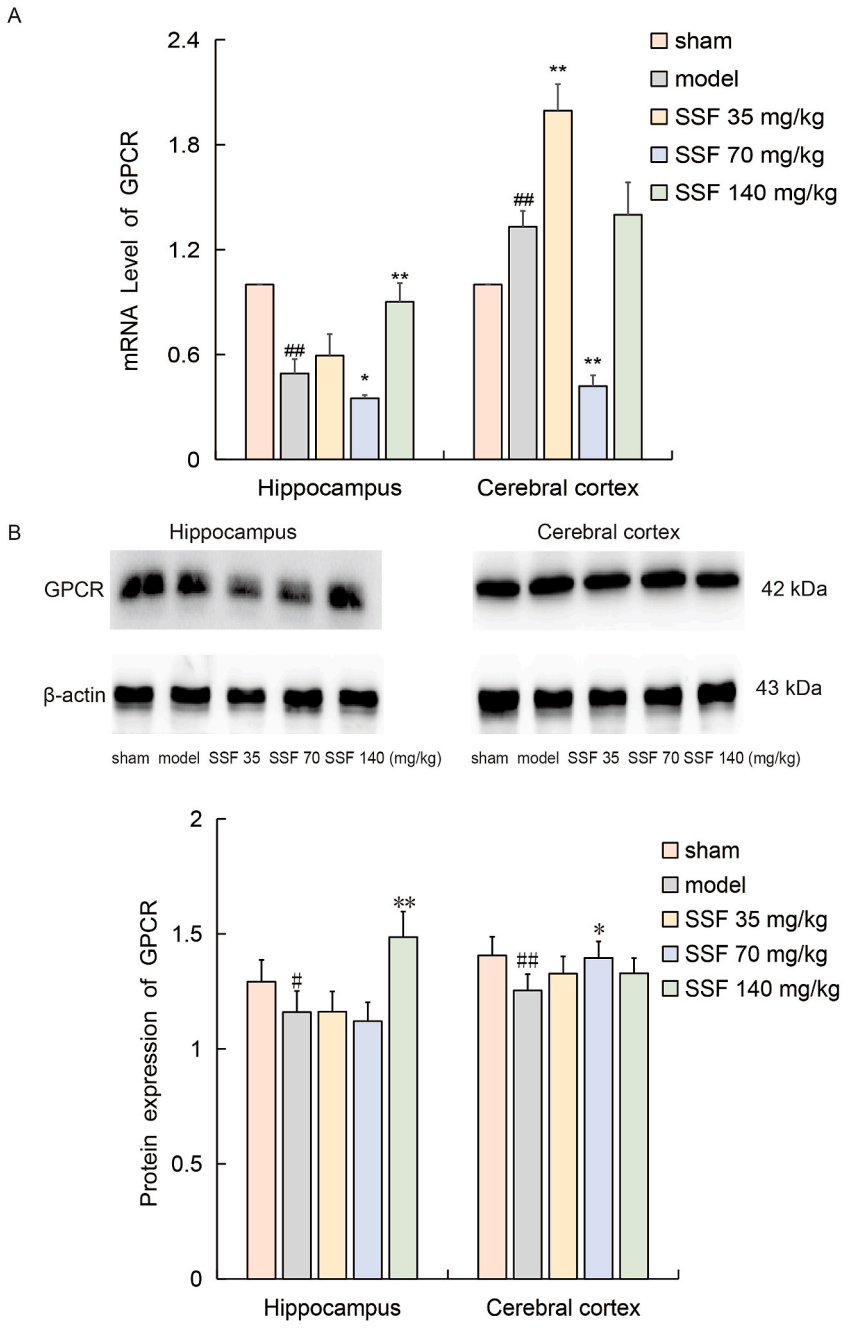

Fig. 7. The influence of SSF on GPCR mRNA (A) and protein (B) expression in rats. Mean ± SD. n = 3. #$P < 0.05$ vs sham group; ##$P < 0.01$ vs sham group; **$P < 0.01$ vs model group; *$P < 0.05$ vs model group.

levels of the Gαs protein. Compared with that in the model group, the expression of the Gαs protein in the hippocampus of the rats increased by 15.51% (35 mg/kg SSF, $P < 0.01$), 27.40% (70 mg/kg SSF, $P < 0.01$) and 4.69% (140 mg/kg SSF, $P > 0.01$). Treatment with 70 mg/kg SSF increased the expression of the Gαs protein in the cerebral cortex by 46.45% ($P < 0.01$). However, 35 mg/kg and 140 mg/kg SSF decreased the expression of the gαs protein in the cerebral cortex by 4.53% ($P < 0.01$) and 29.80% ($P < 0.01$), respectively.

3.10.3. Rat AC1 mRNA and protein expression in response to SSF

According to Fig. 9A, the expression of AC1 mRNA can be seen in the rat hippocampus and cerebral cortex. The model group presented 10.22% (hippocampus, $P > 0.001$) and 63.12% (cerebral cortex, $P > 0.001$) lower AC1 mRNA levels than did the sham

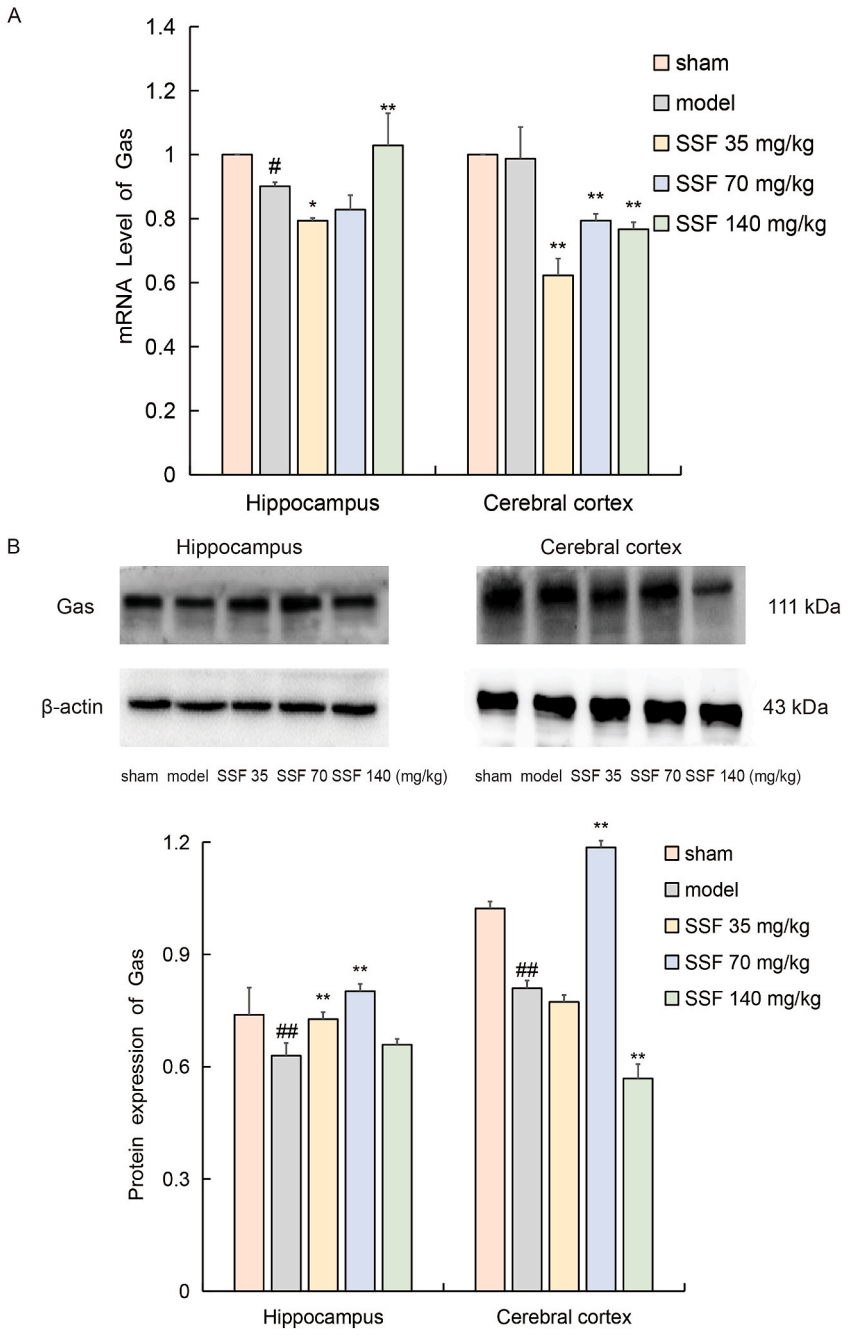

Fig. 8. The influence of SSF on Gαs mRNA (A) and protein (B) expression in rats. A: Gαs mRNA expression, B: Gαs protein expression. Mean ± SD. n = 3. #$P < 0.05$, ##$P < 0.01$ vs sham group; *$P < 0.05$, **$P < 0.01$ vs model group.

group. However, compared with those in the model group, the three different SSF doses increased AC1 mRNA expression in the hippocampus by 18.56% (35 mg/kg SSF, $P < 0.05$) and 21.64% (70 mg/kg SSF, $P < 0.05$) and decreased AC1 mRNA expression by 13.37% (140 mg/kg SSF, $P > 0.05$). On the other hand, AC1 mRNA expression in the cerebral cortex increased by 23.21% (35 mg/kg SSF, $P > 0.05$) and 14.58% (140 mg/kg SSF, $P > 0.05$), whereas it decreased by 29.28% (70 mg/kg SSF, $P < 0.05$).

Fig. 9B shows the differences in the protein expression levels of AC1 in the rats in the different groups. Compared to that in the sham-operated group, AC1 protein expression in the model group was reduced by 11.80% (hippocampus, $P < 0.01$) and 12.81% (cerebral cortex, $P < 0.01$). However, compared with that in the model group, AC1 protein expression in the hippocampus of rats was positively correlated with the dose of SSF after 36 days of gavage of the three doses, which increased by 14.78% ($P < 0.01$), 47.60% ($P < 0.01$), and 37.03% ($P < 0.01$). A Compared with that in the model, AC1 protein expression in the subcortical areas of the brain did

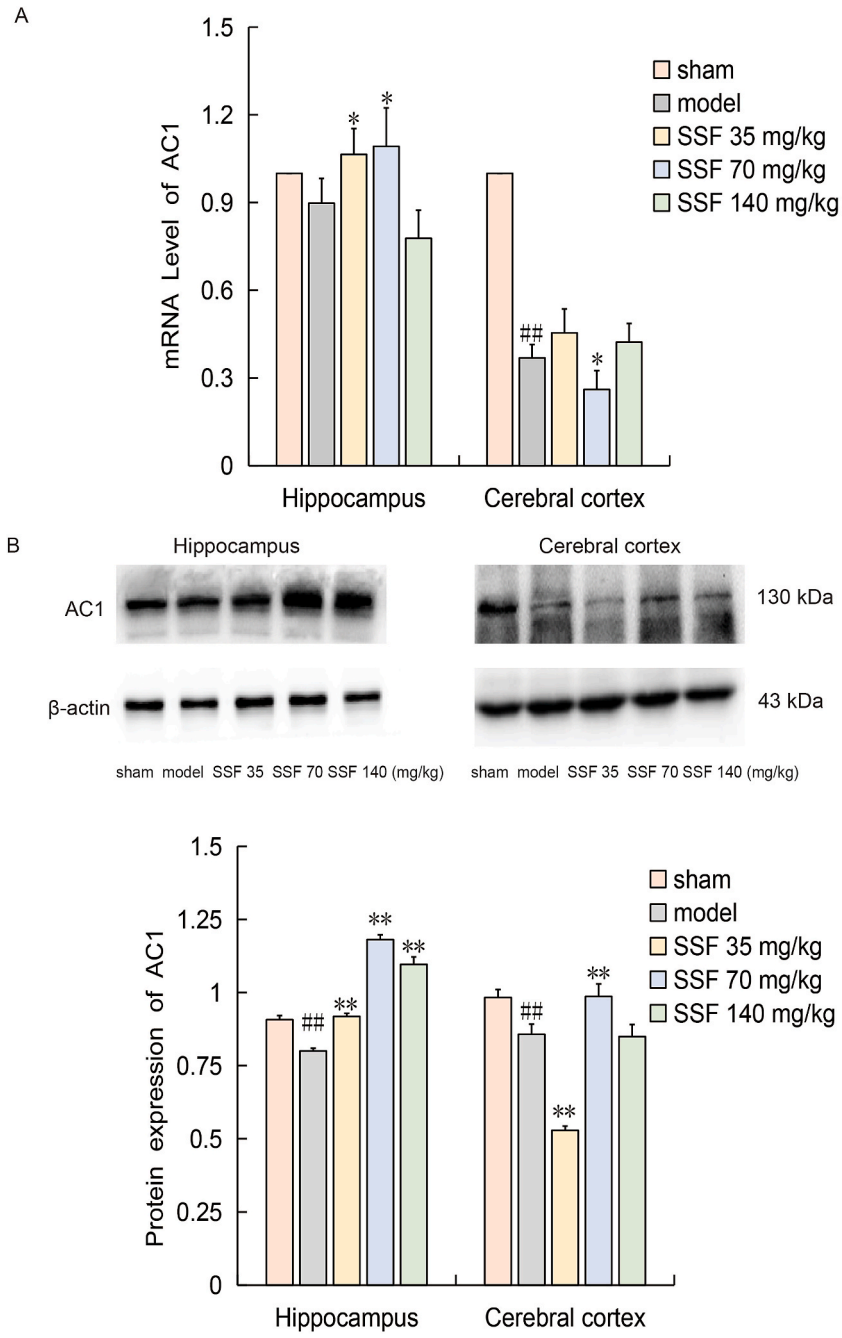

Fig. 9. The influence of SSF on AC1 mRNA (A) and protein (B) expression in rats. Mean ± SD. n = 3. ##$P < 0.01$ vs sham group; *$P < 0.05$, **$P < 0.01$ vs model group.

not increase by 15.07% at 70 mg/kg SSF but decreased by 38.31% ($P < 0.01$) or 0.91% at 35 and 140 mg/kg SSF, respectively.

3.10.4. Rat PKA protein expression in response to SSF

In Fig. 10, shows the PKA protein expression in the rat hippocampal and cerebral cortex regions. Compared with that in the sham group, the PKA protein expression in the model group decreased by 19.93% (hippocampal region, $P < 0.01$) and 22.20% (cerebral cortex, $P < 0.01$). After three different doses of SSF were administered for 36 days, 13.94% ($P < 0.01$) and 1.75% ($P < 0.01$) of the 35 mg/kg and 70 mg/kg SSF-treated groups, respectively, exhibited increased expression of the PKA protein in the hippocampus. Conversely, compared with that in the model group, the protein expression in the SSF 140 mg/kg group was reduced by 7.92% ($P <$

0.05). The experimental groups were treated with 35, 70, or 140 mg/kg SSF, and the PKA protein expression in the cerebral cortex increased by 1.25%, 12.36%, and 6.75%, respectively.

3.10.5. Rat VEGF mRNA and protein expression in response to SSF

As the results in Fig. 11A display, VEGF mRNA expression in rats differed among the groups. Similarly, compared with that in the sham-operated group, the expression of VEGF mRNA in the hippocampal and cortical regions of the model rats was increased by 157.75% ($P < 0.01$) and 56.49% ($P < 0.01$), respectively. Compared to that in the model group, after intragastric administration of three doses of SSF for 36 days, VEGF mRNA expression was reduced by 11.31% (hippocampus, $P > 0.01$) and 26.33% (cerebral cortex, $P < 0.01$) by treatment with 35 mg/kg of SSF and was attenuated by 3.37% (hippocampus, $P > 0.01$) and 32.73% (cerebral cortex, $P < 0.01$) by treatment with 70 mg/kg SSF and was increased by 26.02% (hippocampus, $P < 0.01$) and 18.98% (cerebral cortex, $P < 0.01$) by treatment with 140 mg/kg SSF.

As shown in Fig. 11B, the hippocampus and cortical regions of the rat brain expressed the VEGF protein. The VEGF protein expression was increased by 140.92% ($P < 0.01$) in the hippocampal region and 14.47% ($P < 0.01$) in the cerebral cortex of rats in the model group compared with those in the sham group. A dose-dependent increase in VEGF protein expression in the hippocampus was observed compared with that in the model group at the three different SSF doses. With respect to the dose of SFF administered (35, 70 and 140 mg/kg), VEGF protein expression increased by 58.32% ($P < 0.01$), 18.61% ($P < 0.01$), and 0.17%, respectively. VEGF protein expression was reduced by 26.33% ($P < 0.01$), 32.73% ($P < 0.01$) and 18.98% ($P < 0.01$) in the cerebral cortex by treatment with 35, 70, and 140 mg/kg SSF, respectively.

4. Discussion

Network pharmacology is an interdisciplinary method used to explore the systemic effects of traditional Chinese medicine. By

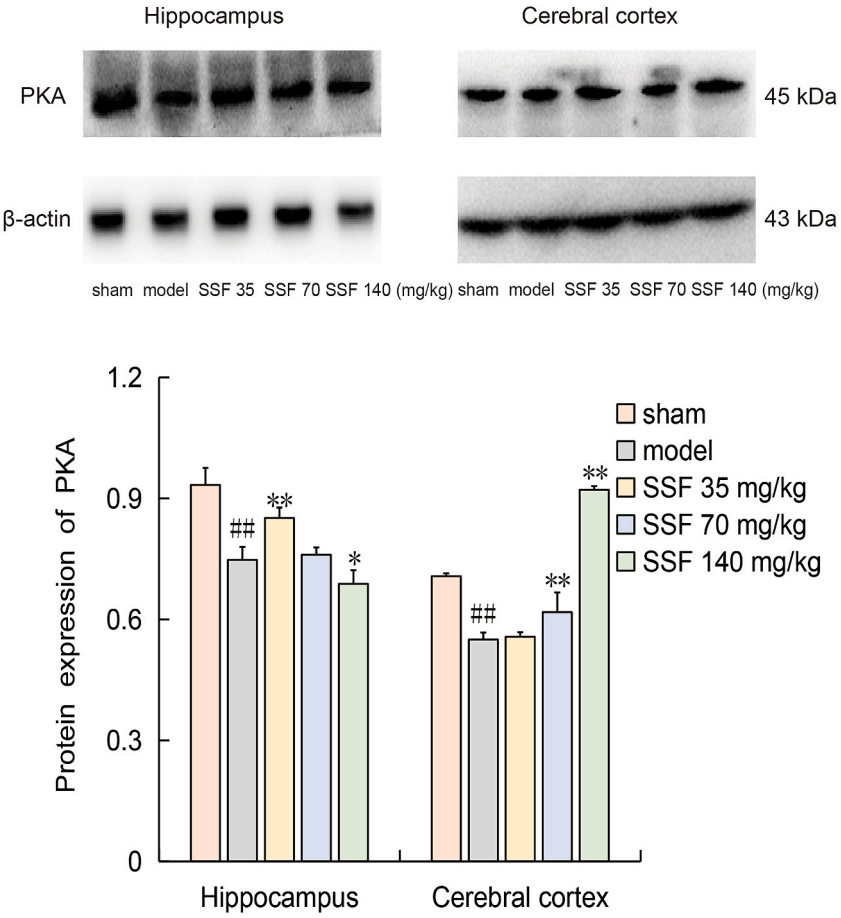

Fig. 10. The influence of SSF on PKA protein expression in rats. Mean ± SD. n = 3. ##$P < 0.01$ vs sham group; *$P < 0.05$, **$P < 0.01$ vs model group.

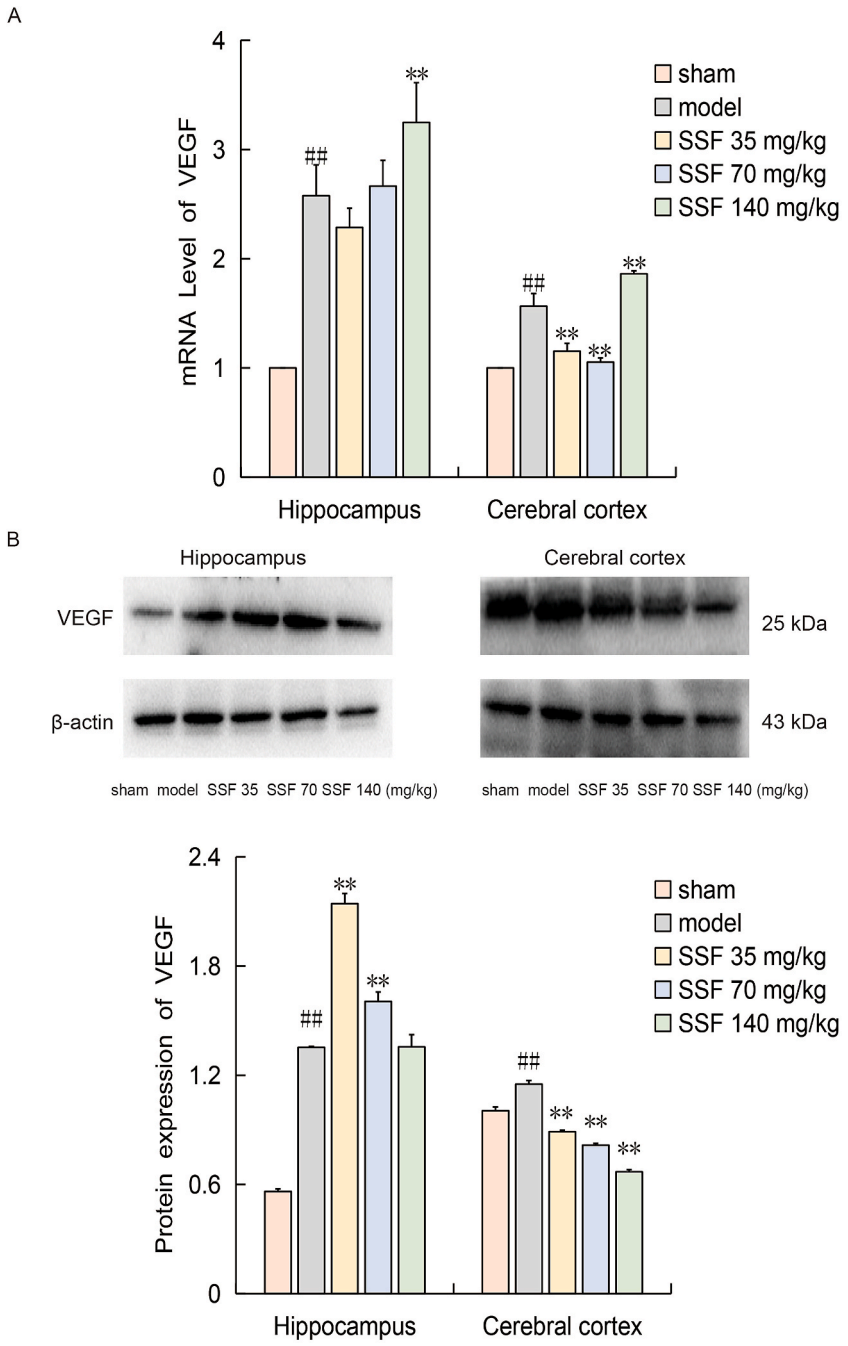

Fig. 11. The influence of SSF on VEGF mRNA (A) and protein (B) expression in rats. Mean ± SD. n = 3. $\#\#P < 0.01$ vs sham group; $**P < 0.01$ vs model group.

combining biology, pharmacology, and bioinformatics, a potential research strategy for discovering the relationship between diseases and active ingredients, including natural small molecules, can be identified [18]. Single-cell transcriptome sequencing can accurately cluster cells, discover new cell types, and study the expression of random genes[29,30]. Bulk RNA-seq can overcome the shortcoming of insufficient sequencing depth in single-cell transcriptome analysis[31]. The amalgamation of the aforementioned three approaches is highly advantageous for facilitating the provision of enhanced precision in drug research and development, as well as for paving the way for novel avenues. This scholarly article discerns the shared targets between AD and SSF by employing pharmaceuticals, two GEO datasets associated with AD, and disease databases. Ultimately, this investigation yielded nine potential drug targets closely linked to the aforementioned conditions, namely APP, CTSB, PIK3R1, IGF1R, PDGFRA, ALK, CALM1, CA2 and DNM1.

In AD rat models, SSF is an anti-neurodegenerative Chinese herbal medicine [12–14,32,33]. However, the molecular mechanism by

which SSF composites inhibit AD has not been determined. Bioinformatics analysis indicated that AD and SSF exhibit overlapping targets that promote inflammation, oxidative stress, and neurodegenerative function. This study identified the cAMP signaling pathway as a relevant signaling pathway according to KEGG enrichment analysis based on the expression of two key genes, PIK3R1 and CALM 1. These findings align with previous findings on the AD signaling pathway. In the article published by our team, the PI3K-AKT signaling pathway was identified as one of the signaling pathways through which SSF affects AD [28]. This article also discusses how PI3K-AKT-CREB signaling promotes neurogenesis and improves memory impairment in rats. Numerous studies have reported a relationship between the cAMP-PKA-CREB signaling pathway and AD progression [34–36]. Moreover, apoptosis in neurons can be reduced by Magnolol, which can activate the cAMP-PKA-CREB pathway and upregulate CHRM1 [36]. There is evidence that DAla2GIP-Glu-PAL improves cognitive behavior, synaptic plasticity, and the pathology in APP/PS1 mice, through the inhibition of neuroinflammation and the upregulation of the cAMP-PKA-CREB pathway[35]. This difference may be due to the stimulation of the cAMP-PKA-CREB-BDNF pathway and the anti-inflammatory effects of FFPM, a new phosphodiesterase-4 inhibitor, which reverses the cognitive impairment of APP/PS1 transgenic mice [34]. Consequently, this paper also showed that the anti-AD effect of SSF is influenced by the cAMP-PKA-CREB pathway.

Notably, GO analysis revealed that the primary biological processes exhibited a strong association with AD. Among the enriched biological process terms, protein autophosphorylation was the most common. Notably, the hyperphosphorylation of the Tau protein is a significant pathological characteristic of AD. Previous research has indicated that SSF ameliorates impaired memory by inhibiting the hyperphosphorylation of the Tau protein at multiple sites, thereby exerting neuroprotective effects [12]. The phosphorylation of proteins is regulated by the genes encoding PKA and CREB in the cAMP signaling pathway [37]. An enriched CC, which includes the myelin sheath, is closely associated with pathological changes in AD, such as Aβ deposition and neurofibrillary tangles. Preventing myelin sheath loss may be an effective strategy for preventing AD [38]. High levels of cAMP hinder myelin regeneration in Schwann cells, but inhibiting cAMP with SSF indirectly protects the myelin sheath [39,40]. These findings align with those of Congcong X et al. [41] Phosphatidylinositol 3-kinase (PI3K) binding is encompassed within the enriched MF terms. The administration of SSF to rats resulted in the activation of the PI3K-AKT-CREB signaling pathway, leading to enhanced memory and the alleviation of neurogenesis disorders. Upregulation of PI3K, AKT, and CREB expression was observed following SSF treatment [28]. Notably, the inhibitory effect of SSF on PI3K and AKT can be attributed to elevated cAMP levels, as G protein-coupled receptors facilitate cAMP upregulation [42]. Consequently, the anti-AD effect of SSF can be attributed to its multi-target and multi-signaling properties.

In patients with AD, a decrease in the number of newborn neurons often occurs alongside learning, memory, and cognitive function disorders. Neuroregeneration has become the primary focus of treatment for central nervous system diseases, particularly AD. Currently, it is widely believed that neuroregeneration occurs in the cerebral cortex, subventricular zone (SVZ), and subgranular zone (SGZ) [43]. Neuroregeneration produces new neurons, which can migrate to the damaged parts of neurons, generate action potentials,

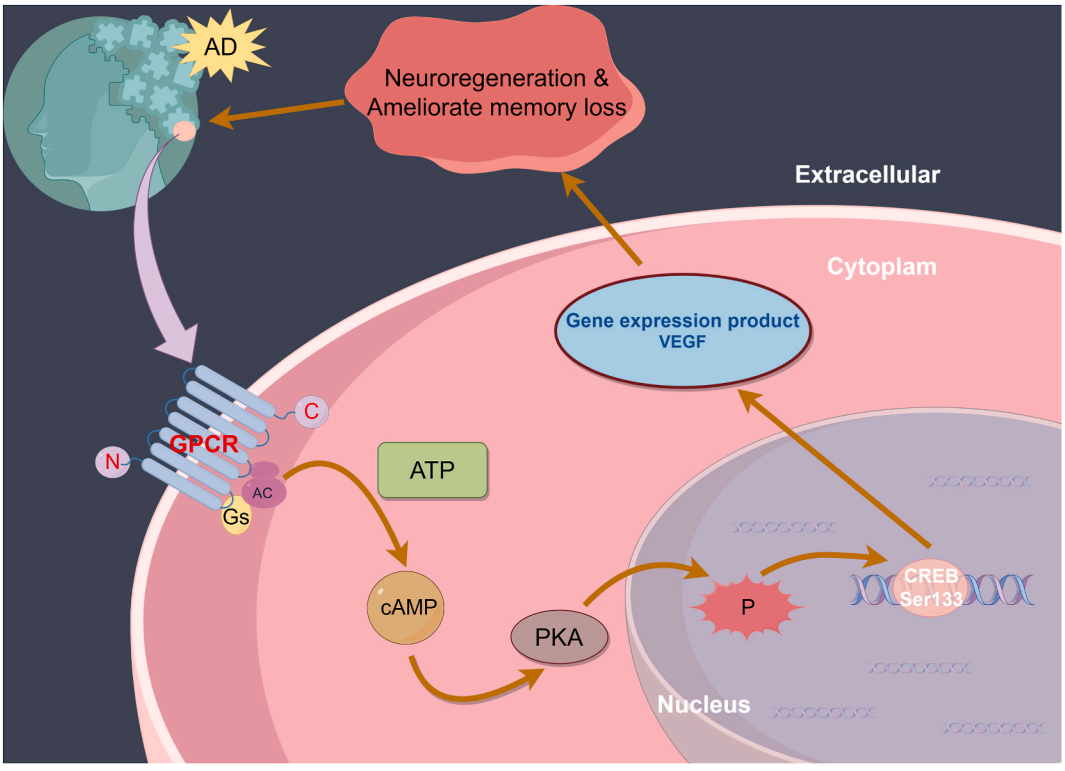

Fig. 12. cAMP-PKA-CREB signaling pathway.

and establish synaptic connections with surrounding neurons to compensate for the damaged nerve structure and function [44]. It has been shown that Brdu can be used instead of thymine deoxynucleoside for the synthesis of DNA during the S phase of the cell cycle. A positive Brdu expression indicates the presence of newly synthesized DNA and is associated with nerve cell proliferation [45].In the laboratory, there are many methods for testing rats' memory abilities, such as the shuttle box experiment, which is a classical combined learning conditioning paradigm. The purpose of the shuttle box test is to assess whether a rat can effectively avoid harmful stimuli through learning, thus reflecting the ability of the rat to learn from conditional stimuli according to the number of harmful stimuli avoided during the incubation period. The present study revealed that intracerebroventricularly administered composited Aβ could increase the positive Brdu expression in the cerebral cortex, reduce the AARR and GARR, and increase the AARL and PARL in rats. However, three doses of SSF (35, 70, and 140 mg/kg) increased the protein expression and positive cells number of Brdu-positive cells and reversed the changes in the AARR, GARR, AARL, and PARL, which paralleled the improvements demonstrated by SSF in terms of neuroregeneration and memory impairment. The results showed that composited Aβ could initiate memory loss in rats, accompanied by a decrease in neuroregeneration. SSF significantly improved the memory loss caused by intracerebroventricular administration of composited Aβ and increased nerve regeneration in the brain. Moreover, the ability of the SSF to ameliorate memory impairment may be related to its ability to promote nerve regeneration.

Several signal transduction pathways regulate neuroregeneration, including the cAMP-PKA-CREB pathway, which is an important pathway that regulates neuroregeneration and memory formation (Fig. 12). Activation of this pathway can promote neuronal survival, regeneration and differentiation and is associated with synaptic plasticity, learning, and memory [46,47], which is highly important for studying neuroregeneration and memory impairment in AD patients. When the extracellular signal stimulates the GPCR receptor on the cell membrane, the GPCR recognizes different ligands and induces G protein activation through GDP and GTP conversion. GPCR coupled with G protein activates AC, AC catalyzes the formation of cAMP, and cAMP can activate PKA. Then, PKA phosphorylates the CREB serine at the position of 133. As illustrated in Fig. 9, phosphorylated CREB regulates the transcription of downstream genes and protein synthesis, enabling the cAMP-PKA-CREB signaling pathway to produce the effects of promote the repair and survival of nerve cells, reduce cell apoptosis, and improve learning and memory impairment[48,49].

GPCR, also known as seven α-helix transmembrane cell surface receptors, regulate various cellular functions by binding to ligands. A number of GPCR members, including Wnt receptors, neuropeptide Y, pituitary adenylate cyclases-activating peptides, and peptides from the intestinal fluid, have been confirmed to promote the proliferation and differentiation of neural stem cells [50]. GPCR results revealed decreased reactivity under repeated extracellular signal stimulation, and the expression of these proteins changed to varying degrees with different durations of ligand treatment. The G protein is composed of α, β and γ subunits, in which the α subunit determines the specificity of the G protein [51]. In AD patients, Gαs is significantly decreased, and its downregulation is positively correlated with pathological severity. There are 10 subtypes of AC, namely, AC1-AC9 and a soluble AC10. The brain and central nervous system express high levels of AC1, which affects synaptic plasticity, memory, and learning. Studies have shown that mice lacking AC1 have obvious long-term memory dysfunction and neurological dysfunction [52,53], and the activity of AC can also reflect the ability of G protein activation. In this study, we found that the intracerebroventricular injection of composite Aβ into rats decreased the expression of the GPCR, Gαs, and AC1 mRNAs and proteins in the hippocampus and cerebral cortex after injection. As a result, complex Aβ disrupts the normal metabolism of the Gαs and AC1 genes and proteins in the brain. However, three doses of SSF regulated the decreases in the mRNA and protein expression of GPCR, Gαs, and AC1, which were induced by composited Aβ to varying degrees and attributed to promotion of neuroregeneration and improvement of memory impairment by SSF. The results indicate that SSF can up-regulate GPCR, Gαs, and AC1 expression, ensuring normal signal transduction via cAMP-PKA-CREB.

cAMP, functioning as a secondary messenger, governs cellular activities. Its production occurs through ATP cyclization, catalyzed by AC under the influence of Gα. The binding level of cAMP is predominantly associated with PKA regulatory subunits. Within the context of learning and memory formation, cAMP actively contributes to the activation of genes implicated in long-term memory and facilitates the synthesis of proteins crucial for the establishment of enduring memory [54]. The activity of PKA depends on the level of intracellular cAMP, and the phosphorylation of CREB depends on PKA activity. When the cAMP concentration and PKA concentration decrease, CREB phosphorylation is inhibited, the expression of molecules related to neuroregeneration and memory formation decreases, and new synapses are disconnected, thus inducing learning and memory impairment [6]. A protein kinase is composed of two catalytic subunits and two regulatory subunits. Once cAMP binds to the regulatory subunit, it activates the free catalytic. Normally, PKA participates in Tau protein phosphorylation. When the activity of PKA is down-regulated due to a decrease in the AC level or G-protein coupling disorder, Tau protein is hyperphosphorylated. The PKA pathway is also involved in the metabolism of amyloid precursor protein (APP). A functional defect in PKA pathway decreases the secretion of the APP α enzyme and accelerates deposition of Aβ[55]. PKA inhibitors can not only inhibit the transduction of the cAMP-PKA-CREB signaling pathway in the brain but also cause serious damage to the long-term memory in the brain[56]. The results of this study showed that intracerebroventricular injection of composited Aβ decreased the production of cAMP and down-regulated the PKA protein expression in the hippocampus and cerebral cortex regions of rat brains. However, three doses of SSF reversed decreases in cAMP and PKA levels, which were induced by composited Aβ in rats to varying degrees. It appears that SSF improved neuroregeneration and memory deficits in these animals. Earlier studies have shown that SSF may enhance brain CREB-Ser133-phosphorylated gene and protein expression [57], suggesting that SSF could up-regulate the expression of cAMP and PKA in the cAMP-PKA-CREB signaling pathway, promote CREB-Ser133 phosphorylation, and induce downstream functional protein transcription, thereby playing a role in neuronal regeneration, synaptic formation, learning, and memory.

VEGF is a downstream gene in the cAMP-PKA-CREB signaling pathway. Vascular endothelial cells are specifically stimulated to proliferate and maintain their function when they are administered. Additionally, VEGF can nourish nerve cells, protect nerves, and promote neuroregeneration directly [58]. In the brain tissue of patients with AD, researchers have shown that VEGF can compensate

for the effects of low perfusion and neuronal apoptosis by promoting neuroangiogenesis, neuronutrition, and neuroprotection [59,60]. Loss of neurons and degeneration of cerebral vessels can induce memory impairment in AD patients. In the early stage of AD, VEGF can antagonize vascular hypoxia perfusion, slow down neurovascular injury and clear Aβ deposition, and temporarily increase the expression of VEGF. With the aggravation of the course of AD, the increased reactivity of VEGF was decreased, the injury of vascular functional integrity was aggravated, and the expression of VEGF was decreased [61–63]. Additionally, in vitro studies have demonstrated that VEGF might be involved in neuroregeneration and could significantly increase the number of BrDU-labeled newborn neurons [64]. After intracerebroventricular administration of the Aβ composite, VEGF mRNA and protein expression were significantly increased in the hippocampus and cerebral cortex of rats. However, there were differences in VEGF mRNA and protein expression among the three doses of SSF. It is inferred that rats intracerebroventricularly administered composited Aβ showed a compensatory increase in VEGF expression, and treatment with SSF could promote the Brdu protein expression to play a crucial role in neuroregeneration.

In summary, this study identified the key targets and signaling pathways of SSF in AD, indicating that SSF is a promising multitarget drug for the treatment of AD. The inhibitory effect and mechanism of action of SSF on AD were verified in animal models, providing a new perspective and basis for clinical research on the transformation of Chinese herbal medicines. However, some remaining problems related to our research limitations must be solved. First, the information from the online database is based on reviewed and predicted data. Therefore, these unconfirmed and unrecorded compounds or targets may not be included in our analysis. Second, the quantitative determination of 21 compounds is currently incomplete. The sample may include some unidentified components. Therefore, research on content determination should be carried out in the future. Third, further research is needed to determine the absorption route, effective components, significant effective components, and metabolic forms of bioactive substances in SSF. This is because the results of this study have not been verified in actual AD patients. Therefore, in the future, we will further clarify the potential mechanism of action of SSF in AD through the combination of multiple omics methods and determine the safety and effectiveness of SSF in treating AD.

5. Conclusion

In conclusion, the findings of this study indicate that SSF has the potential to enhance the expression of the Brdu protein, improve memory impairment, and promote neuroregeneration in the presence of composited Aβ. Additionally, SSF has been shown to upregulate the mRNA and protein expression levels of Gαs, AC1, cAMP, PKA, and VEGF in the cAMP-PKA-CREB signaling pathway. Previous research has also demonstrated that SSF can increase the expression of p-CREB-Ser133 by upregulating both the mRNA and protein levels. Consequently, SSF can facilitate neuroregeneration and alleviate memory impairment through the regulation of the cAMP-PKA-CREB signaling pathway.

Ethical approval statement

All animal experiments were conducted according to the Regulations of Experimental Animal Administration issued by the State Committee of Science and Technology, China on Oct. 31, 1988. The study was approved by the Animal Ethics Committee of Chengde Medical University under the serial number CDMULAC-20190226-002.

Data availability

Data supporting the results of this study can be obtained from the corresponding authors.

Funding

This project was supported by Hebei Provincial Education Department of Graduate Student Innovation Ability Training (No. CXZZSS2020124), Hebei Provincial Natural Science Foundation, China (No. H2019406063); Hebei Provincial Administration of Traditional Chinese Medicine (No. 05027, 2014062); Hebei Provincial Education Department (No. ZD20131022, ZD2019057); Leading Subject of Chengde Medical College; Advantage Subject of Chengde Medical College; Science and Technology Innovation Team Construction Project of Chengde Medical University, China. (No.(2020) 50).

CRediT authorship contribution statement

Yinhui Yao: Writing – original draft, Software, Methodology, Investigation, Data curation. **Qianqian Liu:** Methodology, Investigation. **Shengkai Ding:** Resources, Methodology. **Yan Chen:** Software, Methodology. **Tangtang Song:** Software, Resources. **Yazhen Shang:** Writing – review & editing, Supervision, Project administration, Formal analysis, Conceptualization.

Declaration of competing interest

The authors declare that they have no known competing financial interests or personal relationships that could have appeared to influence the work reported in this paper.

Appendix A. Supplementary data

Supplementary data to this article can be found online at https://doi.org/10.1016/j.heliyon.2024.e27161.

References

[1] Y. Hase, T.M. Polvikoski, M.J. Firbank, L.J.L. Craggs, E. Hawthorne, C. Platten, W. Stevenson, Small vessel disease pathological changes in neurodegenerative and vascular dementias concomitant with autonomic dysfunction, Brain Pathol. 30 (1) (2020) 191–202.
[2] D. Eratne, S.M. Loi, S. Farrand, W. Kelso, D. Velakoulis, J.C. Looi, Alzheimer's disease: clinical update on epidemiology, pathophysiology and diagnosis, Australas. Psychiatr. 26 (4) (2018) 347–357.
[3] J.A. Soria Lopez, H.M. González, G.C. Léger, Alzheimer's disease, Handb. Clin. Neurol. 167 (2019) 231–255.
[4] D. Julian, E.W. Hollingsworth, K. Julian, J. Imitola, Convergence of human cellular models and genetics to study neural stem cell signaling to enhance central nervous system regeneration and repair, Semin. Cell Dev. Biol. 95 (2019) 84–92.
[5] A.R. Wang, M.Z. Hu, Z.L. Zhang, Z.Y. Zhao, Y.B. Li, B. Liu, Fastigial nucleus electrostimulation promotes axonal regeneration after experimental stroke via cAMP/PKA pathway, Neurosci. Lett. 699 (2019) 177–183.
[6] X. Gao, X. Zhang, L. Cui, R. Chen, C. Zhang, J. Xue, L. Zhang, Ginsenoside Rb1 promotes motor functional recovery and axonal regeneration in post-stroke mice through cAMP/PKA/CREB signaling pathway, Brain Res. Bull. 154 (2020) 51–60.
[7] X.R. Han, X. Wen, Y.J. Wang, S. Wang, M. Shen, Z.F. Zhang, S.H. Fan, Effects of CREB1 gene silencing on cognitive dysfunction by mediating PKA-CREB signaling pathway in mice with vascular dementia, Mol. Med. 24 (1) (2018) 18.
[8] Y. Qiu, Y. Wang, X. Wang, C. Wang, Z.Y. Xia, Role of the hippocampal 5-HT1A receptor-mediated cAMP/PKA signalling pathway in sevoflurane-induced cognitivedysfunction in aged rats, J. Int. Med. Res. 46 (3) (2018) 1073–1085.
[9] Y.S. Zhu, Y.F. Xiong, F.Q. Luo, J. Min, Dexmedetomidine protects rats from postoperative cognitive dysfunction via regulating the GABA(B) R-mediated cAMP-PKA-CREB signaling pathway, Neuropathology 39 (1) (2019) 30–38.
[10] H. Liao, J. Ye, L. Gao, Y. Liu, The main bioactive compounds of Scutellaria baicalensis Georgi. for alleviation of inflammatory cytokines: a comprehensive review, Biomed. Pharmacother. 133 (2021) 110917.
[11] G. Liu, N. Rajesh, X. Wang, M. Zhang, Q. Wu, S. Li, B. Chen, Identification of flavonoids in the stems and leaves of Scutellaria baicalensis Georgi, J. Chromatogr., B: Anal. Technol. Biomed. Life Sci. 879 (13–14) (2011) 1023–1028.
[12] D. Shengkai, S. Yazhen, Flavonoids from stems and leaves of Scutellaria baicalensis Georgi regulate the brain tau hyperphosphorylation at multiple sites induced by composited Aβ in rats, CNS Neurol. Disord.: Drug Targets 21 (4) (2022) 367–374.
[13] X. Congcong, Y. Yuanyuan, L. Caixia, S. Yazhen, The Effects and Mechanism of Scutellaria baicalensis Georgi Stems and Leaves Flavonoids on Myelin Sheath Degeneration Induced by Composite Aβ in Rats, CNS Neurol Disord Drug Targets 23 (4) (2024) 504–511.
[14] H. Zhang, Q.Q. Liu, S.K. Ding, H. Li, Y.Z. Shang, Flavonoids from stems and leaves of Scutellaria baicalensis Georgi improve composited aβ-induced Alzheimer's disease model rats' memory and neuroplasticity disorders, Comb. Chem. High Throughput Screen. 26 (8) (2023) 1519–1532.
[15] H. Chen, J. Zhao, J. Hu, X. Xiao, W. Shi, Y. Yao, Y. Wang, Identification of diagnostic biomarkers, immune infiltration characteristics, and potential compounds in rheumatoid arthritis, BioMed Res. Int. 2022 (2022) 1926661.
[16] Y. Yao, J. Zhao, J. Hu, H. Song, S. Wang, W. Ying, Identification of potential biomarkers and immune infiltration in pediatric sepsis via multiple-microarray analysis, Eur. J. Inflamm. 20 (2022), 1721727X221144392.
[17] G.A. Altê, A.L.S. Rodrigues, Exploring the molecular targets for the antidepressant and antisuicidal effects of ketamine enantiomers by using network pharmacology and molecular docking, Pharmaceuticals 16 (7) (2023).
[18] Z. Song, P. Gao, X. Zhong, M. Li, M. Wang, X. Song, Identification of five hub genes based on single-cell RNA sequencing data and network pharmacology in patients with acute myocardial infarction, Front. Public Health 10 (2022) 894129.
[19] A. Daina, O. Michielin, V. Zoete, SwissTargetPrediction: updated data and new features for efficient prediction of protein targets of small molecules, Nucleic Acids Res. 47 (W1) (2019) W357–w364.
[20] A. Grubman, G. Chew, J.F. Ouyang, G. Sun, X.Y. Choo, C. McLean, R.K. Simmons, A single-cell atlas of entorhinal cortex from individuals with Alzheimer's disease reveals cell-type-specific gene expression regulation, Nat. Neurosci. 22 (12) (2019) 2087–2097.
[21] S. Zeng, L. Chen, X. Liu, H. Tang, H. Wu, C. Liu, Single-cell multi-omics analysis reveals dysfunctional Wnt signaling of spermatogonia in non-obstructive azoospermia, Front. Endocrinol. 14 (2023) 1138386.
[22] W.S. Liang, T. Dunckley, T.G. Beach, A. Grover, D. Mastroeni, D.G. Walker, R.J. Caselli, Gene expression profiles in anatomically and functionally distinct regions of the normal aged human brain, Physiol. Genom. 28 (3) (2007) 311–322.
[23] P. Langfelder, S. Horvath, WGCNA: an R package for weighted correlation network analysis, BMC Bioinf. 9 (2008) 559.
[24] G. Yu, L.G. Wang, Y. Han, Q.Y. He, clusterProfiler: an R package for comparing biological themes among gene clusters, OMICS 16 (5) (2012) 284–287.
[25] D. Szklarczyk, J.H. Morris, H. Cook, M. Kuhn, S. Wyder, M. Simonovic, A. Santos, The STRING database in 2017: quality-controlled protein-protein association networks, made broadly accessible, Nucleic Acids Res. 45 (D1) (2017) D362–d368.
[26] Y. Shang, J. Cheng, J. Qi, H. Miao, Scutellaria flavonoid reduced memory dysfunction and neuronal injury caused by permanent global ischemia in rats, Pharmacol. Biochem. Behav. 82 (1) (2005) 67–73.
[27] W. Xiaoguang, C. Jianjun, C. Qinying, Z. Hui, Y. Lukun, S. Yazhen, Establishment of a valuable mimic of Alzheimer's disease in rat animal model by intracerebroventricular injection of composited amyloid beta protein, J. Vis. Exp. 137 (2018).
[28] Q.Q. Liu, S.K. Ding, H. Zhang, Y.Z. Shang, The molecular mechanism of Scutellaria baicalensis Georgi stems and leaves flavonoids in promoting neurogenesis and improving memory impairment by the PI3K-AKT-CREB signaling pathway in rats, Comb. Chem. High Throughput Screen. 25 (5) (2022) 919–933.
[29] S.S. Potter, Single-cell RNA sequencing for the study of development, physiology and disease, Nat. Rev. Nephrol. 14 (8) (2018) 479–492.
[30] R. Huang, M. Xu, W. Guo, M. Cheng, R. Dong, J. Tu, S. Xu, Network pharmacology and experimental verification-based strategy for exploring the mechanisms of luteolin in the treatment of osteosarcoma, Cancer Cell Int. 23 (1) (2023) 213.
[31] S. Picelli, Single-cell RNA-sequencing: the future of genome biology is now, RNA Biol. 14 (5) (2017) 637–650.
[32] G. Miao, H. Zhao, K. Guo, J. Cheng, S. Zhang, X. Zhang, Z. Cai, Mechanisms underlying attenuation of apoptosis of cortical neurons in the hypoxic brain by flavonoids from the stems and leaves of Scutellaria baicalensis Georgi, Neural Regen. Res. 9 (17) (2014) 1592–1598.
[33] D. Shengkai, L. Qianqian, S. Yazhen, The effects and regulatory mechanism of flavonoids from stems and leaves of Scutellaria baicalensis Georgi in promoting neurogenesis and improving memory impairment mediated by the BDNF-ERK-CREB signaling pathway in rats, CNS Neurol. Disord.: Drug Targets 21 (4) (2022) 354–366.
[34] H. Guo, Y. Cheng, C. Wang, J. Wu, Z. Zou, B. Niu, H. Yu, FFPM, a PDE4 inhibitor, reverses learning and memory deficits in APP/PS1 transgenic mice via cAMP/PKA/CREB signaling and anti-inflammatory effects, Neuropharmacology 116 (2017) 260–269.
[35] L. Yuan, J. Zhang, J.H. Guo, C. Holscher, J.T. Yang, M.N. Wu, Z.J. Wang, DAla2-GIP-GLU-PAL protects against cognitive deficits and pathology in APP/PS1 mice by inhibiting neuroinflammation and upregulating cAMP/PKA/CREB signaling pathways, J Alzheimers Dis 80 (2) (2021) 695–713.
[36] G. Zhu, Y. Fang, X. Cui, R. Jia, X. Kang, R. Zhao, Magnolol upregulates CHRM1 to attenuate Amyloid-β-triggered neuronal injury through regulating the cAMP/PKA/CREB pathway, J. Nat. Med. 76 (1) (2022) 188–199.
[37] H. Zhang, Q. Kong, J. Wang, Y. Jiang, H. Hua, Complex roles of cAMP-PKA-CREB signaling in cancer, Exp. Hematol. Oncol. 9 (1) (2020) 32.

[38] L.R. Hirschfeld, S.L. Risacher, K. Nho, A.J. Saykin, Myelin repair in Alzheimer's disease: a review of biological pathways and potential therapeutics, Transl. Neurodegener. 11 (1) (2022) 47.
[39] R.P. Lisak, B. Bealmear, L. Nedelkoska, J.A. Benjamins, Secretory products of central nervous system glial cells induce Schwann cell proliferation and protect from cytokine-mediated death, J. Neurosci. Res. 83 (8) (2006) 1425–1431.
[40] K.R. Jessen, R. Mirsky, The repair Schwann cell and its function in regenerating nerves, J. Physiol. 594 (13) (2016) 3521–3531.
[41] X. Congcong, Y. Yuanyuan, L. Caixia, S. Yazhen, The effects and mechanism of Scutellaria baicalensis Georgi stems and leaves flavonoids on myelin sheath degeneration induced by composite Aβ in rats, CNS Neurol. Disord.: Drug Targets 23 (4) (2024) 504–511.
[42] S.E. Desale, H. Chidambaram, S. Chinnathambi, G-protein coupled receptor, PI3K and Rho signaling pathways regulate the cascades of Tau and amyloid-β in Alzheimer's disease, Mol. Biomed. 2 (1) (2021) 17.
[43] G.L. Ming, H. Song, Adult neurogenesis in the mammalian brain: significant answers and significant questions, Neuron 70 (4) (2011) 687–702.
[44] C. Hollands, N. Bartolotti, O. Lazarov, Alzheimer's disease and hippocampal adult neurogenesis; exploring shared mechanisms, Front. Neurosci. 10 (2016) 178.
[45] Y.L. Zhang, S.D. Qiu, P.B. Zhang, W. Shi, BrdU-labelled neurons regeneration after cerebral cortex injury in rats, Chin. Med. J. 119 (12) (2006) 1026–1029.
[46] M.M. Siddiq, S.S. Hannila, Looking downstream: the role of cyclic AMP-regulated genes in axonal regeneration, Front. Mol. Neurosci. 8 (2015) 26.
[47] N.J. Batty, K.K. Fenrich, K. Fouad, The role of cAMP and its downstream targets in neurite growth in the adult nervous system, Neurosci. Lett. 652 (2017) 56–63.
[48] S. Shnitkind, M.A. Martinez-Yamout, H.J. Dyson, P.E. Wright, Structural basis for graded inhibition of CREB:DNA interactions by multisite phosphorylation, Biochemistry 57 (51) (2018) 6964–6972.
[49] J.E. Lee, W.J. Song, H. Lee, B.G. Kim, T. Kim, C. Lee, B. Jang, AniScan using extracellular cyclic AMP-dependent protein kinase A as a serum biomarker assay for the diagnosis of malignant tumors in dogs, Sensors 20 (15) (2020).
[50] V.A. Doze, D.M. Perez, G-protein-coupled receptors in adult neurogenesis, Pharmacol. Rev. 64 (3) (2012) 645–675.
[51] Y. Huang, T. Rafael Guimaräes, N. Todd, C. Ferguson, K.M. Weiss, F.R. Stauffer, B. McDermott, G protein-biased GPR3 signaling ameliorates amyloid pathology in a preclinical Alzheimer's disease mouse model, Proc. Natl. Acad. Sci. U. S. A. 119 (40) (2022) e2204828119.
[52] L.L. Susick, J.L. Lowing, K.E. Bosse, C.C. Hildebrandt, A.C. Chrumka, A.C. Conti, Adenylyl cylases 1 and 8 mediate select striatal-dependent behaviors and sensitivity to ethanol stimulation in the adolescent period following acute neonatal ethanol exposure, Behav. Brain Res. 269 (2014) 66–74.
[53] X. Liu, Y. Zhou, D. Yang, S. Li, X. Liu, Z. Wang, Type 3 adenylyl cyclase in the MOE is involved in learning and memory in mice, Behav. Brain Res. 383 (2020) 112533.
[54] N.H. Woo, T. Abel, P.V. Nguyen, Genetic and pharmacological demonstration of a role for cyclic AMP-dependent protein kinase-mediated suppression of protein phosphatases in gating the expression of late LTP, Eur. J. Neurosci. 16 (10) (2002) 1871–1876.
[55] N.S. Kron, L.A. Fieber, Aplysia neurons as a model of Alzheimer's disease: shared genes and differential expression, J. Mol. Neurosci. 72 (2) (2022) 287–302.
[56] D. Byers, R.L. Davis, J.A. Kiger Jr., Defect in cyclic AMP phosphodiesterase due to the dunce mutation of learning in Drosophila melanogaster, Nature 289 (5793) (1981) 79–81.
[57] H. Zhang, S.K. Ding, Q.Q. Liu, Y.Y. Ye, Q. Xu, Y.Z. Shang, Ca2+-Camk-CREB mediates the effect of flavonoids from Scutellaria baicalensis stems and leaves on the decrease of neuroregeneration-induced by composited Aβ in rats, Int. J. Med. Plants and Natural Products 5 (4) (2019) 18–28.
[58] K. Jin, Y. Zhu, Y. Sun, X.O. Mao, L. Xie, D.A. Greenberg, Vascular endothelial growth factor (VEGF) stimulates neurogenesis in vitro and in vivo, Proc. Natl. Acad. Sci. U. S. A. 99 (18) (2002) 11946–11950.
[59] H. Tayler, J.S. Miners, Ö. Güzel, R. MacLachlan, S. Love, Mediators of cerebral hypoperfusion and blood-brain barrier leakiness in Alzheimer's disease, vascular dementia and mixed dementia, Brain Pathol. 31 (4) (2021) e12935.
[60] M.A. Tubi, D. Kothapalli, M. Hapenney, F.W. Feingold, W.J. Mack, K.S. King, P.M. Thompson, Regional relationships between CSF VEGF levels and Alzheimer's disease brain biomarkers and cognition, Neurobiol. Aging 105 (2021) 241–251.
[61] P. Wang, Z.H. Xie, Y.J. Guo, C.P. Zhao, H. Jiang, Y. Song, Z.Y. Zhu, VEGF-induced angiogenesis ameliorates the memory impairment in APP transgenic mouse model of Alzheimer's disease, Biochem. Biophys. Res. Commun. 411 (3) (2011) 620–626.
[62] P. Religa, R. Cao, D. Religa, Y. Xue, N. Bogdanovic, D. Westaway, H.H. Marti, VEGF significantly restores impaired memory behavior in Alzheimer's mice by improvement of vascular survival, Sci. Rep. 3 (2013) 2053.
[63] R. Parodi-Rullán, J. Ghiso, E. Cabrera, A. Rostagno, S. Fossati, Alzheimer's amyloid β heterogeneous species differentially affect brain endothelial cell viability, blood-brain barrier integrity, and angiogenesis, Aging Cell 19 (11) (2020) e13258.
[64] K.L. Jin, X.O. Mao, D.A. Greenberg, Vascular endothelial growth factor: direct neuroprotective effect in in vitro ischemia, Proc. Natl. Acad. Sci. U. S. A. 97 (18) (2000) 10242–10247.